UCRL-LR-131000

Inner-Shell Photoionized X-Ray Lasers

S. J. Moon
(Ph.D. Dissertation)

September 1998

Work performed under the auspices of the U.S. Department of Energy by Lawrence Livermore National Laboratory under Contract W-7405-ENG-48.

UCRL-LR-131000
Distribution Category UC-0

Inner-Shell Photoionized X-Ray Lasers

S. J. Moon
(Ph.D. Dissertation)

September 1998

LAWRENCE LIVERMORE NATIONAL LABORATORY
University of California • Livermore, California • 94551

Inner-Shell Photoionized X-Ray Lasers

by

Stephen J. Moon

B.S. (California State Polytechnic University, Pomona) 1990
M.S. (San Jose State University) 1992

A dissertation submitted in partial satisfaction of the
requirements for the degree of
Doctor of Philosophy

in

Engineering, Applied Science

in the

GRADUATE DIVISION
of the
UNIVERSITY of CALIFORNIA at DAVIS

Committee in charge:

Professor C. William McCurdy, Chair
David C. Eder, Ph.D.
Professor John De Groot

The dissertation of Stephen J. Moon is approved:

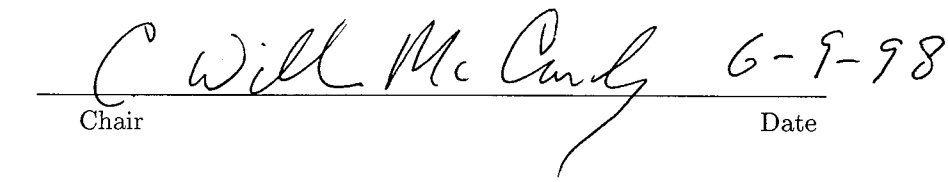

Chair Date

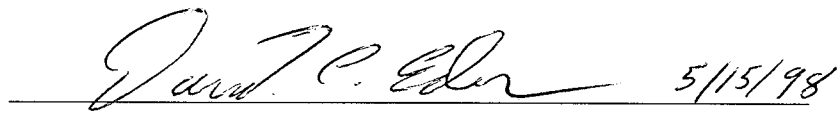

Date

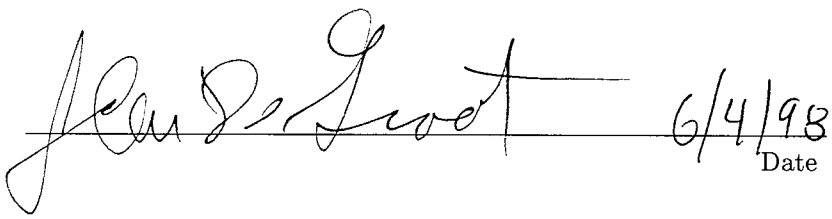

Date

University of California at Davis

1998

Inner-Shell Photoionized X-Ray Lasers

Dedicated to

Debora and Ivan

and

In loving memory of,

Patricia Jane Moon

(1925-1996)

Contents

List of Figures

List of Tables

Acknowledgements

I would like to thank my advisors: David Eder, Bill McCurdy and John De Groot. My technical advisor David Eder has helped me understand what it is to be a researcher. I am indebted to him and I count myself fortunate to have met him and his family. Bill McCurdy has been the perfect advisor. He is a wonderful teacher and an understanding person. John De Groot has not only helped guide my career, but engaged me in many interesting conversations on a great diversity of subjects. I am constantly amazed with the breadth and depth of his knowledge. Rich London, Chris Decker, Mordy Rosen, Luiz DaSilva, Rich Snavely, Ed Alley, Bruce Young, Al Osterheld, Mau Chen and all those who work in X-division.

I wish to thank Doug McColm and Jonathan Heritage for asking tough questions and requiring me to think on my feet.

I am indebted to my teachers past and present. In particular I want to thank Ann Orel for teaching me Atomic Physics, Fred Wooten for his Prep Class, Roger Haas for teaching me Lasers, Gary Rodrigue for teaching me Advanced Numerical Methods, Roger Dodd for his friendship and for his introduction to the world of Chaos, and Peter Siegel, a past advisor and friend, for steering me into this realm of science. They have given me the gift of their time and knowledge.

I have been given the opportunity to attend graduate school through the generous financial support of the Student-Employee program at Lawrence Livermore National Laboratory. I could not have succeeded in this program without the help of Bill Chandler and the support of the Student Policy Committee. The Student-Employee program is a

wonderful program and I recommend it to all.

My office mate Hank Alme has contributed to this thesis in several ways, the most important has been *coffee*. To Wally Kaechele and Darryl Allen, with whom I spent many late night hours studying, thank you for the time and for making my first year of graduate school tolerable. To the Historical Society of DAS for archiving some of the most infamous events which transpired during my tenure.

I also, am indebted to my son Ivan for his humor and imagination. Foremost I must acknowledge my wife Debora. It has been through her patience and tolerance of my passion for physics and my desire to do research that I have been able to pursue my dream.

Stephen John Moon
September, 1998
Engineering - Applied Science

Abstract

Inner-Shell Photoionized X-Ray Lasers

by

Stephen J. Moon

Doctor of Philosophy in Engineering, Applied Science

University of California at Davis

Professor C. William McCurdy, Chair

The inner-shell photoionized x-ray lasing scheme is an attractive method for achieving x-ray lasing at short wavelengths, via population inversion following inner-shell photoionization (ISPI). This scheme promises both a short wavelength and a short pulse source of coherent x rays with high average power. In this dissertation a very complete study of the ISPI x-ray laser scheme is done concerning target structure, filter design and lasant medium. An investigation of the rapid rise time of x-ray emission from targets heated by an ultra-short pulse high-intensity optical laser was conducted for use as the x-ray source for ISPI x-ray lasing.

Lasing by this approach in C at a wavelength of 45 Å requires a short pulse (about 50 fsec) driving optical laser with an energy of 1–5 J and traveling wave optics with an accuracy of $\sim$ 15μm. The optical laser is incident on a high-Z target creating a high-density plasma which emits a broadband spectrum of x rays. This x-ray source is passed

through a filter to eliminate the low-energy x rays. The remaining high-energy x rays preferentially photoionize inner-shell electrons resulting in a population inversion. Inner-shell photoionized x-ray lasing relies on the large energy of a K-α transition in the initially neutral lasant. The photon energy required to pump this scheme is only slightly greater than the photon energy of the lasing transition yielding a lasing scheme with high quantum efficiency. However, the overall efficiency is reduced due to low x-ray conversion efficiency and the large probability of Auger decay yielding an overall efficiency of $\sim 10^{-7}$ resulting in an output energy of μJ's. We calculate that a driving laser with a pulse duration of 40 fs, a 10μm $\times$ 1 cm line focus, and an energy of 1 J gives an effective gain length product (gl) of 10 in C at 45 Å. At saturation ($gl \sim 18$) we expect an output of $\sim 0.1\mu$J per pulse. The short duration of x-ray lasing (< 100 fs) combined with a 10-Hz repetition rate ($P_{\text{avg}} = 1\mu$W) makes this source of coherent x rays ideal for pump-probe experiments to study fast dynamical processes in chemistry and material science.

Professor C. William McCurdy
Dissertation Committee Chair

Chapter 1

Introduction

Since the successful demonstration of x-ray lasing by Dennis Matthews, et al. [1] in 1984 the number of researchers involved in x-ray laser research has grown and advancements in the field of x-ray lasers and x-ray laser applications have been dramatic. High power Nova-class lasers have produced x-ray lasing reliably and achieved high pulse energies needed for many imaging applications. Prepulse techniques have been exploited and optimized to achieve higher efficiencies. Currently, the achievement of x-ray lasing is common place and quite reliable.

The original focus of the x-ray laser community was to achieve x-ray lasing with mJ energy per pulse within the water window (44 Å – 24 Å) in order to produce a hologram of cells in solution and then to continue the push towards shorter wavelengths with the intent to image finer structure finally resolving atoms and molecules. The possibility of the Ni-like collisional scheme to achieve lasing within the water window has been demonstrated at 35 Å in Au [2] however saturation was not achieved. Saturation has been demonstrated

at a wavelength of 73 Å at RAL [3] thus placing the initial goal of high power x-ray lasing within sight. However, for many other applications a single large x-ray pulse is not needed as much as very short duration pulses with a high average power, i.e., high repetition rate.

A table-top chirped pulse amplification (CPA) laser driver with short pulse width and a few joules of energy can produce x-ray lasing and offer a high repetition rate. Current work using the JANUS laser at LLNL to pump a transient collisional excitation scheme by Jim Dunn, et al. has shown lasing in Ni-like Pd at 147 Å [4]. This scheme produces a short-pulse high repetition rate x-ray laser. However, lasing is on the order of picoseconds which is too long for some applications and the extension of this scheme to wavelengths shorter than $\sim$ 23 Å will be difficult. To achieve lasing at very short wavelengths alternatives must be investigated. One difficulty with the collisional schemes is the large amount of energy required to sufficiently ionize the atom to achieve the desired lasing transition. Lasing on an inner-shell transition eliminates the need to produce a highly charged ion. Another difficulty is the prohibitive per shot expense for the large Nova-class lasers. A table-top system would drastically reduce this expense and help speed along the time between experiments. One approach to table top x-ray lasing which offers both a short pulse and short wavelength is by inner-shell photoionization in an originally neutral low-Z atom, such as carbon. This x-ray lasing scheme takes advantage of the K-α transition to achieve lasing at x-ray wavelengths. This thesis investigates the possibility of x-ray lasing by means of inner-shell photoionization and determines the regime where lasing can be achieved.

1.1 Conventional X-Ray Lasers

Conventional x-ray lasing requires a large optical laser to produce the needed plasma conditions to achieve x-ray lasing. There are only a handful of lasers around the world with the required energy to drive a conventional Ne-like or Ni-like x-ray laser. Plasma conditions necessary to achieve x-ray lasing require kJ's of energy and the first demonstrated x-ray laser by Matthews, et al. [1] used two beams of the Nova Laser incident on a Se foil to produce Ne-like Se where lasing took place on the 3p to 3s collisionally pumped transition. Since that time tremendous progress has taken place at several major research laboratories around the world.

The researchers at the Laboratoire d'Utilisation des Lasers Intenses (LULI, Palaiseau, France) have shown reliable x-ray lasing in Ne-like Zn at 212 Å, using their 0.45 kJ, 600 ps pulse driving laser with a wavelength of 1.06 μm. The lasing takes place on a $3p - 3s$ J = 0–1 transition with an output energy of $E_{out} \sim 1$ mJ [5]. X-ray lasing is consistently achieved and this laser can be used as a reliable research tool. However, using the large LULI laser limits repetition to a maximum of 30 shots per day. This is one of the major limitations with the use of large laser systems. Researchers at the ASTERIX facility in Germany have demonstrated the effectiveness of the pre-pulse technique and significantly improved the efficiency [6]. The use of a prepulse has been demonstrated as the most effective means of achieving high efficiency in the collisional scheme. The Rutherford Appleton Laboratory (RAL) has achieved saturation in Ne-like Ge at 196 Å [7] and recently at 73 Å in Ni-like Sm [3]. RAL continues to push the limits achieving saturation at shorter and shorter wavelengths, yet saturation within the water window has still to be demonstrated.

Although, these large laser facilities have achieved remarkable success the extension of the collisional x-ray laser scheme to wavelengths below 35 Å will be difficult. The Ne-like and the Ni-like schemes are only capable of achieving lasing down to 23 Å [8]. Further development of these large-scale systems is needed with the possibility of achieving mJ pulses within the water-window (44 Å to 24 Å). However, with the limitation in achieving x-ray lasing below 23 Å the development of other schemes is necessary. Additionally, the large cost of building and maintaining these large lasers limits the researcher. A true table-top x-ray laser is needed and a dedicated x-ray laser facility where researchers could further develop x-ray lasers and associated x-ray laser applications would be helpful.

1.2 Table-Top X-ray Lasers

In the past several years tabletop x-ray lasing has not only become a reality, but also the clear direction for future x-ray lasers. These lasers are relatively inexpensive to build and maintain. They also can provide a high repetition rate in which research can rapidly progress. Increasingly, the use of ultra short pulse (USP) lasers are being investigated as a means to pump x-ray lasers. There are three major approaches being considered. These include optical field ionization (OFI), transient collisional excitation and inner-shell photoionization (ISPI). Optical field ionization utilizes the large electric field induced by a high intensity USP laser which can rapidly remove electrons from an atom. The energy of the ionized electrons depend on their binding energy and the wavelength and pulse shape of the ionizing laser. Lasing has been observed at 135 Å in H-like Li with a relatively small gain-length [9, 10, 11, 12] and in C- and N-like O at 374 and 617 Å,

respectively, with also a small gain-length [13]. In some of these experiments, it appears that ionization induced refraction is limiting the lasing length and thus the gain-length product that can be obtained. A high-gain length product ($gl = 11$) has been observed following field ionization at 418 Å in Xe [14]. At densities for which this collisional Xe laser operates, ionization induced refraction is not a serious problem. However, when this scheme is extended to shorter wavelengths which require higher densities, refraction will become a serious problem. The transient scheme uses collisional ionization where peak gain occurs early in the ionization process when there is an abundance of the lasing ions, e.g., Ne- or Ni-like ions. As the plasma passes through this ionization stage, the electron temperature and the gain coefficient are much higher than that of steady state. The ISPI scheme is a two-step approach to x-ray lasing involving the x-ray photoionization of inner-shell electrons. the first step is to produce a pulse of incoherent x rays with a very rapid rise time by heating a high-Z material with an USP laser. In the second step, a low energy filter removes x rays that could ionize outer-shell electrons and the remaining x rays primarily ionize inner-shell electrons. This approach has not been demonstrated at x-ray wavelengths but modeling shows that lasing at 45 Å is possible with existing USP lasers and down to 15 Å with planned USP laser drivers.

Within the last 5 years there have been major advances in obtaining high optical intensity through chirped pulse amplification. Pulse duration as short as 20 fs [15, 16] and powers > 1 PW, with longer pulse duration ($\sim$500 fs), have been demonstrated [17, 18]. The repetition rate for these USP lasers depends on the total energy per pulse. Lasers with energies of order 1 J have been operated at repetition rates of 10 Hz. Using an USP driver,

x-ray lasing at long wavelengths, ($\lambda = 326$ & 418Å) [19, 20] has been demonstrated and there has been some evidence for lasing at somewhat short wavelength ($\lambda \sim 135$Å) [9, 21, 22]. Recent work by Jim Dunn, et al. [23] demonstrated x-ray lasing via the transient scheme in Ni-like Pd at 147 Å.

For wavelengths down to $\sim$ 67 Å [24] there is a mechanism to produce short duration ($\leq$ 100 fs) coherent x rays using high harmonics. Experiments in material science have shown the usefulness of such a short pulse of coherent x rays [25]. However, high harmonics have a very low efficiency of conversion at short wavelengths [26]. RAL has investigated the use of high harmonics generating the 37th harmonic at a wavelength of 67.2 Å [24]. However, the use of harmonics is limited due to the cutoff of the conversion plateau at photon energies lower than ($E_i + 3U_p$) and the inclusion of all higher order odd harmonics in the spectrum.

Direct excitation of the gain medium by a pulsed discharge promises high efficiencies. A Na Z-pinch plasma was used to pump an x-ray laser. This was first successfully demonstrated by producing a population inversion in He-like Ne resonantly photo pumped from the Na $1s^2 - 1s2p\ ^1P_1$ transition [27]. However, the turn-on time of these devices is on the order of ns and USP x-ray lasing can not be achieved by this method. In addition, x-ray lasing in the Z-pinch plasma poses problems due to plasma non-uniformity. Electron-capillary discharge has circumvented this problem by confining the plasma to a small capillary and XUV lasing has been demonstrated at Colorado State University by J. J. Rocca and coworkers who first achieved lasing on the J=0–1 line in Ne-like Ar at 468.8 Å and have recently achieved saturation with a gl of 25 by the use of a pulsed discharge

[28, 29]. This table-top laser has a high efficiency of $\sim 10^{-5}$. However, extension of this scheme to shorter wavelengths will be difficult and require a new approach and a large amount of energy.

Efficiencies in the Ne-like and Ni-like collisional scheme can also be enhanced by the use of a transient gain region [30]. This method has also made it possible to use a high intensity USP optical laser as a pump achieving rapid ionization and a transient region of positive gain. At LLNL the use of the USP high intensity laser JANUS has been used to extend the transient collisional scheme to shorter wavelengths [23] and this scheme can achieve lasing within the water-window [31].

With the development of USP lasers with pulse widths less than 50 fs the inner-shell photoionization x-ray laser scheme is now a exciting method of achieving x-ray lasing with a wavelength below 50 Å. This scheme meets both the USP and the short wavelength requirements.

1.3 Inner-Shell Photoionization X-ray Lasing

In this approach, an energetic incoherent x-ray source with a fast rise time is used to selectively ionize inner-shell electrons of the lasant material. A large K-shell pump rate is needed to compete with the fast Auger decay rate and a fast x-ray rise time is needed to outpace the L-shell collisional ionization. Electron induced ionization from energetic electrons emitted from both photoionization and Auger decay to the lower-laser state limits the magnitude and duration of positive gain. The energy spectrum of the photoionized electrons is dependent on the x-ray source. In the lasing medium, electrons come from both

photoionization and from Auger decay. If the rise time of the x rays is rapid enough, lasing can be achieved before significant electron ionization can occur.

An USP ($\Delta t \leq 50$ fs) optical laser with energy ≥ 1 J is needed to produce a hot plasma at line focus with the required rise time and flux to pump the ISPI x-ray lasant. The plasma generates a broad-band x-ray spectrum with a rapid rise time. A low-Z filter is sandwiched between the target plasma and the lasant to stop a majority of the low energy x rays that can ionize outer-shell electrons and thus populate the lower-laser state. The remaining high energy x rays primarily photo ionize the inner-shell electrons of the lasant atoms. This produces population inversion and resulting positive gain for an allowed 2p-1s radiative transition in the singly charged ion for a sufficiently intense x-ray source. A rapid Auger decay of the 1s hole state competes with the lasing transition and produces a large number of energetic electrons into the lasant material. Also, electron induced ionization to the lower state limits the magnitude and duration of positive gain. Ultra-short pulse x-ray lasing is inherent in this scheme.

The scheme was originally proposed by Duguay and Rentzepis [32] but problems of collisional ionization associated with the relatively long pulse optical lasers available at that time caused x-ray lasing to never be realized. More recent work, using an assumed blackbody source with a specified rise time, done by Kapteyn [33] and Strobel, et al. [34] concentrated on very short wavelengths, $\lambda \leq 15$Å, where x-ray lasing has not been demonstrated. In their work they showed that Ne and Mg can be used as lasants given a sufficiently energetic source with a fast rise time.

In this work it has been my goal to determine the needed energy and pulse width

of the optical driving laser in order to achieve x-ray lasing in C. For the low-Z elements C has the minimum requirement on pump energy and thus can be used as a proof-of-principle for the ISPI x-ray laser scheme. This dissertation concentrates on the requirements for ISPI x-ray lasing in C at 45Å and demonstrates that the fast rise-time requirements can be met by an USP laser-produced plasma. An investigation of the rapid rise time of incoherent x-ray emission from targets heated by an USP high-intensity optical laser is conducted for use as the x-ray source for ISPI x-ray lasing. Previous studies considered front-side x-ray emission; however, ISPI x-ray lasing requires a filtered x-ray source. Modeling using the hydrodynamics/atomic kinetics code LASNEX [35] of a 40 fs USP driving laser with an intensity of $10^{17}\mathrm{W/cm}^2$ incident on a flat target of thin Au layered on a Be filter is presented. The filter has a modest influence on the x-ray emission of the Au via conduction cooling but has a large effect on the backside spectrum by removing low energy x rays as the Au emission passes through the filter. The use of such a filtered source is shown to provide the needed energy to produce a significant gain-length product in C. Therefore, current laser systems can produce a laser-produced plasma source with the incoherent x-ray flux and rise-time demands such that x-ray lasing in C can be achieved.

Chapter 2

Inner-Shell Photoionization X-Ray Lasing

This chapter gives a description of the inner-shell photoionized (ISPI) x-ray laser scheme for low-Z elements and requirements to achieve lasing. Section 2.1 presents an overview of the ISPI x-ray laser scheme. A simple calculation is performed to determine the necessary conditions to achieve lasing and the saturated output energy expected. In section 2.2 a time dependent blackbody source is used to perform gain calculations for various low-Z elements using a specified pulse width in order to determine the pump energy requirements needed to achieve x-ray lasing.

2.1 Schematics of ISPI X-Ray Lasing

In the inner-shell photoionization approach to achieve x-ray lasing an inner-shell electron must be ejected by means of photoionization. A K-shell hole is created so that an

allowed 2p-1s radiative transition can take place, described by the equation,

$$C + h\nu \rightarrow C^{+}[K] + e$$

where [K] represents an $n = 1$ or K-shell vacancy. An energetic photon will preferentially photo ionize an inner-shell electron and in this way a population inversion can be achieved on the 2p-1s transition. However, there is a competing non-radiative Auger transition that can fill this K-shell hole leaving a doubly ionized ion in an LL state. This idea was first discussed by Duguay and Rentzepis [32] over 30 years ago and it has proven difficult to achieve lasing due to the fast competing non-radiative Auger transition and destructive collisional excitation to the lower-laser state. However, by the use of a fast rise time pumping source these limitations can be overcome and x-ray lasing can be achieved. In addition, the K-L lasing transition has a narrow energy width and for low-Z elements, $Z \leq 20$. The transition KL to LL poses an additional problem for high-Z elements however for low-Z elements the difference in the energy between the KL to LL transition and the energy of the K to L lasing transition is larger than the transition width. However, for elements with $Z > 20$ this is not the case and radiative trapping of the lasing transition will destroy this scheme.

As seen in Fig. 2.1 an x-ray source creates a K-shell hole in carbon where an allowed K to L (2p-1s) radiative transition can take place yielding a 45Å photon. For x rays above the K-shell energy only a small fraction $\leq 5\%$ of the ionizations are out of the L shell. Therefore the possibility arises for inversion between C^{+} states with K- and L-shell holes. However, the dominant decay channel out of the upper-laser state is a non-radiative Auger transition to C^{++}, with a lifetime of 10.3 fs compared to the radiative

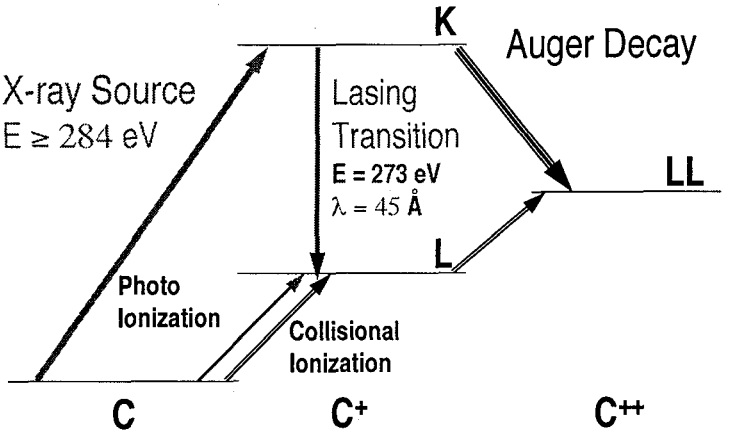

Figure 2.1: A rate equation diagram for inner-shell photoionization x-ray lasing in C at 45Å. A high energy x-ray photon can preferentially photo ionize an inner-shell electron creating a K-shell hole where a K-L shell transition can take place.

lifetime of 1230 fs [36]. Both photoionization and an Auger transition produce a population of energetic free electrons. These electrons can ionize an L-shell electron in the neutral atom and populate the lower-lasing state. Consequently, the pump must have a fast rise time to achieve significant population inversion before electron ionizations destroy the inversion.

2.1.1 Rate Equations

From the basic energy level diagram shown in figure 2.1 we can construct a simple set of rate equations. A detailed set of rate equations used in our numerical model of ISPI x-ray lasing are described in Appendix A. The laser rate equations in the small signal approximation are given below.

$$\dot{\mathrm{N}}_0 = -(R_K + R_L + R_{Le})\mathrm{N}_0 \tag{2.1}$$

$$\dot{\mathrm{N}}_K = R_K \mathrm{N}_0 - \frac{\mathrm{N_K}}{\tau_\mathrm{K}} \tag{2.2}$$

$$\dot{\mathrm{N}}_L = (R_L + R_L^e)\mathrm{N}_0 - (\mathrm{R_{LL}} + \mathrm{R_{LL}^e})\mathrm{N_L} + \frac{\mathrm{N_K}}{\tau_\mathrm{Rad}} \tag{2.3}$$

$$\mathrm{g} = \sigma_s \left(\mathrm{N_K} - \frac{\mathrm{g_K}}{\mathrm{g_L}} \mathrm{N_L} \right) \tag{2.4}$$

where the gain is denoted g, the degeneracies of the upper- and lower-laser levels are denoted g_K and g_L, respectively and σ_s is the stimulated emission cross section. Here the photoionization and electro ionization rate are R_i and R_i^e respectively, where $i \in \{K, L, LL\}$. The photoionization and electro ionization rates are given by:

$$R_i = \int_0^\infty dE\ \sigma_i(E)\Phi(E) \tag{2.5}$$

$$R_i^e = \int_0^\infty dE\ \sigma_i^e(E) N_e(E) v_e(E), \tag{2.6}$$

where σ_i and σ_i^e are the photoionization and electro ionization cross section respectively. Φ is the flux of the incoherent pump source, $N_e(E)$ is the number density of electrons with energy between E and dE and $v_e(E)$ their respective velocity. The lifetime of the upper-laser state, both radiative and non-radiative, is given by,

$$\frac{1}{\tau_K} = \frac{1}{\tau_\mathrm{Rad}} + \frac{1}{\tau_\mathrm{Auger}} \tag{2.7}$$

where Rad and Auger refer to radiative and non-radiative transitions out of the K-shell, (see table 2.1). In addition to the laser rate equations we also keep track of the free electrons and their energy distribution as well as secondary electron ionization. These electrons are assumed to be either the result of photoionization or Auger decay. The Auger electron's energy is, $E_K - 2E_L$, resulting from the difference in the K-L transition and the binding energy of the ejected electron.

Element	g_K	g_L	τ_{Auger} (fs)	τ_{Rad} (fs)
C	6	6	10.3	1230
N	3	9	7.0	510
O	18	20	4.6	550
Ne	2	6	2.7	150
Na	2	6	2.3	93
Mg	2	6	2.0	61
Al	2	6	1.9	41
Si	2	6	1.7	28

Table 2.1: Atomic parameters for low-Z elements [36, 37].

2.1.2 Source Requirement Estimate

We can estimate the requirement of the incoherent x-ray source rise time and intensity by simple arguments. The rise time of the x-ray source is determined primarily by the rise time of the USP pump. Assuming a rise time, collisional ionization considerations restrict the neutral density, which combined with a desired gain coefficient determines the needed intensity. The time scale of collisional events is given by $\tau \sim 1/N_0\sigma_{\mathrm{Le}}v$, where N_0 is the neutral density, σ_{Le} is the L-shell electron ionization cross section, and v is the average electron velocity. To have a time scale greater than 50 fs requires a neutral density of less than $10^{20}\mathrm{cm}^{-3}$, using a representative electron thermal velocity corresponding to 100 eV. This density combined with the pump rate (cross section times x-ray flux), $\sigma_{\mathrm{K}}\Phi$, and the Auger lifetime, τ_{Auger}, enable us to estimate the required source intensity. To do so, we assume that lasing takes place before any collisional effects occur and that photoionization

of the L-shell by the filtered x-ray source is negligible. We can approximate the lower-lasing state as empty (numerical calculations throughout this thesis do not make this assumption) and the laser gain as

$$g = \sigma_s N_K \approx \sigma_s(\sigma_K \Phi N_0 \tau_{Auger})$$

where σ_s is the stimulated emission cross section. Absorption of the lasing transition scales linearly with density and will reduce the gain by 4.5cm^{-1} for a neutral density of 10^{20}cm^{-3}. This absorption leads to ionization of the L-shell, yet the photoionizations of the 2s electrons are dominant leading to a small depletion of the neutral density and very little additional population of the lower-lasing level. An effective gain coefficient, accounting for absorption, of 10cm^{-1} requires an x-ray flux of $\sim 10^{29}\text{photons/(sec cm}^2)$ using the neutral density of 10^{20}cm^{-3} and using one-half of the peak K-shell cross section, σ_K (assuming an average photon energy $\approx$ 400 eV). Thus, we have shown in order to limit collisional ionization of the lower-laser state, with an assumed source rise time of 50 fs, a neutral density of $\sim 10^{20}\text{cm}^{-3}$ is required. When coupled to the desire to have gains $> 10\text{cm}^{-1}$ this leads to a requirement that the x-ray source be $> 10^{29}\text{photons/(sec cm}^2)$ or $> 10^{13}\text{W/cm}^2$ for representative photons above the K-shell. For a faster rising source there will be a reduction in the required intensity associated with a higher allowed neutral density.

2.1.3 Output Energy Estimate

A laser heated high-density plasma can be used as an incoherent x-ray source to provide the needed flux and rise time of x rays determined above. Given the calculated gain coefficient, a line source of x rays with a length of order 1 cm is required in order to

have a gain-length product of order 10. Gain-length, gl, products between 5 and 10 provide clear evidence of lasing. To estimate the input laser energy needed to heat the plasma and the output energy on saturation, we assume a line focus of 10μm $\times$ 2cm. The x-ray flux calculated above of 10^{13}W/cm^2 with a duration of 50 fs translates into a requirement of 10^{-3} J of incoherent x rays near the K-shell energy. Detailed calculations in section 4.2 show that a laser produced plasma produces a broad band x-ray source with an x-ray conversion efficiency of 5% while only 2% of these x rays are at energies with appreciable K-shell cross section. Our simple estimate assumes no population in the lower-laser state but detailed calculations in section 2.2 show that including the lower state results in a factor of approximately 2 higher flux requirement. This results in conversion efficiencies of 5×10^{-4} or $\sim$ 2 J of laser energy. We calculate a saturation intensity, $I_{\rm sat} = 4 \times 10^{12}$W/cm^2, with a gain length product (gl) of 18. Using a gain duration of $\sim$ 50 fs, an assumed area of 10μm $\times$ 10μm yields an x-ray laser energy output of $\sim 0.2\mu$J [38]. Thus, the conversion efficiency from optical laser to x-ray laser energy is estimated to be approximately 5×10^{-8}.

2.2 Gain Calculations using a Time-Dependant Blackbody Source

A blackbody source is used here to give a simple and effective test of the inner-shell scheme. For the time dependence of the x-ray source we use a simple expression appropriate for a sech^2 driving pulse [33]. Expressed in terms of a blackbody temperature it is given by

the equation,

$$T_{bb} = T_{\max}\left[\frac{0.881544}{\tau}\int_{-\infty}^{t}\operatorname{sech}^2\left(1.76t'/\tau\right)\mathrm{dt}'\right]^{\frac{4}{9}} \tag{2.8}$$

where τ is the FWHM of the driving laser and $T_{\max}$ is the maximum temperature (this model assumes no cooling). The time-dependent temperature curve is shown in fig. 2.2 for $T_{\max} = 200$ eV and $\tau = 50$ fsec which are appropriate parameters for C. The corresponding gain curve in fig. 2.2 is for a neutral C density of $1.0 \times 10^{20}\mathrm{cm}^{-3}$. The x-ray source is taken to have a transverse extent of 10 μm used in conjunction with a 0.5 μm LiH filter. As shown in fig. 2.2, the gain has a FWHM of $\approx$ 38 fsec, showing the ultra-short pulse nature of this scheme. In fig. 2.3, the corresponding populations of the upper- and lower-laser states are plotted with the filtered intensity of the x-ray source. From this plot we can see that the upper-laser state population follows the intensity of the incoherent source. This is expected given the fast Auger exit channel out of the upper state and will be the case unless the intensity changes on a time scale faster than the inverse of the Auger rate which for C is 10.3 fsec. The lower-laser state population grows exponentially due to electron ionizations.

Previous work [33, 34] has shown that for gains of order $10\mathrm{cm}^{-1}$ in Ne, a maximum blackbody temperature of order 500 eV with rise time of 50 fsec is required. We find that for C a much reduced blackbody temperature ($T_{bb} \approx 200$ eV), with the same 50 fsec rise time, gives comparable gains. Neutral Ne having a closed L shell makes it a good candidate for ISPI lasing, yet current lasers can not provide the needed energy to produce a significant gain-length product in Ne [33]. Because of the open L shell structure in C, it is relatively easier to both collisionally- and photo-ionize the L shell thus destructive filling of the lower-lasing state is more severe for C than Ne. Due to the lower energy requirements for K-shell

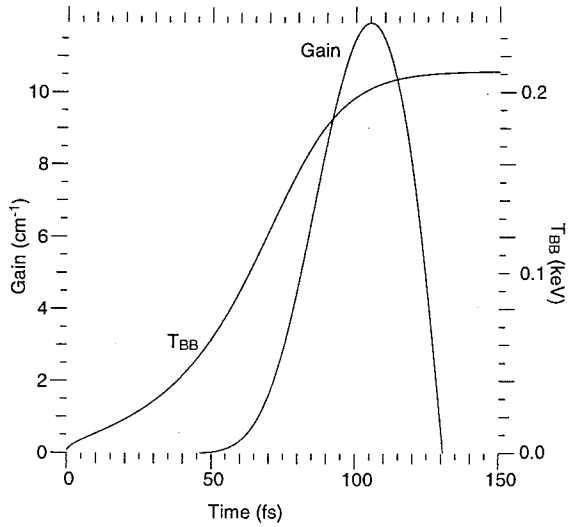

Figure 2.2: A gain coefficient of 12.5cm^{-1} with FWHM = 38 fsec is shown for C with $T_{\max}$ = 200 eV time dependent blackbody source.

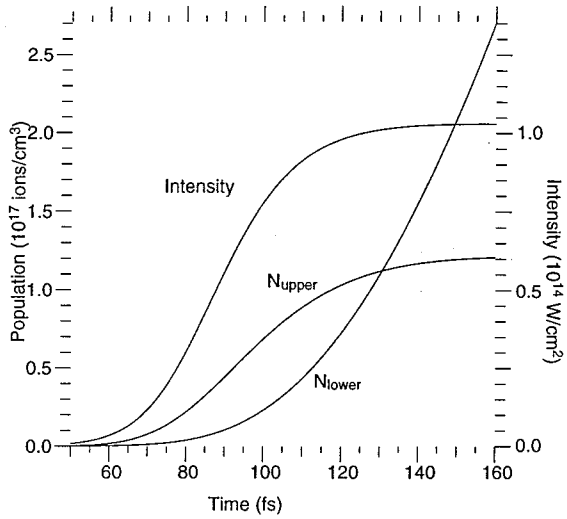

Figure 2.3: Time dependent plots of the upper- and lower-laser state populations leading up to max. gain are shown along with the filtered intensity of the source.

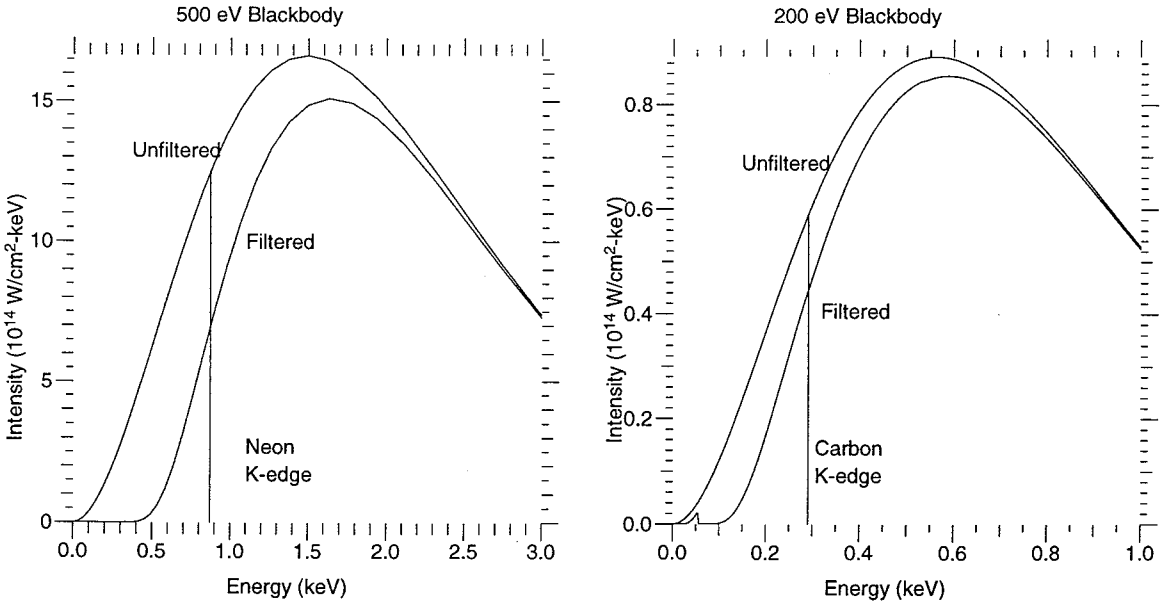

Figure 2.4: X-Ray source requirements for both Ne at 15 Å and C at 45 Å. The filtered source for Ne uses a 3.5 μm Be filter and for C a 0.5 μm LiH filter is used.

ionization of C and the smaller Auger rate the requirement on the intensity of the pump is reduced as compared to Ne; however, the rise time requirements are not changed. Shown in fig. 2.4 are blackbody spectrums appropriate for Ne and C. The filtered spectrum is also shown with the K edge marked for reference. As can be seen for both Ne and C the peak of the filtered spectrum is to the right of the K edge allowing the broad-band nature of the filtered spectrum to be taken advantage of. However, the cross section decays rapidly from its maximum value at the K edge, for example, in C at the peak of the filtered spectrum the cross section is 1/4 of its K-edge value, whereas the filtered spectrum only increases by a factor of 2 above its K-edge value. This results in the convolution of the intensity and the absorption cross section having a peak very near the K edge and decreasing monotonically for higher energies. The replacement of the broad-band source with a line source near the K edge or a band of emission above the K edge would reduce the requirements on the source. For a line source at the K edge the flux required for the x-ray source is approximately 1/6 that of the 200 eV broad-band source.

I have investigated several low-Z elements to determine the needed pump energy to achieve ISPI x-ray lasing. In table 2.2 I show selected low-Z elements along with their ISPI x-ray lasing wavelength. The laser rate equations were solved for various T_{max} and filter thickness and the minimum value of T_{max} for a gain $> 10cm^{-1}$ was determined. The approximate pump energy was determined by the relation,

$$T \propto \Phi^{4/9}\tau^{-2/9} \tag{2.9}$$

described by Caruso and Gratton [39] for a laser-produced plasma where T is the blackbody temperature, Φ is the flux and τ is the laser pulse width. In table 2.2 the laser

Element	Lasing Wavelength Å	T_{max} for gain $> 10cm^{-1}$ (eV)	Approx. Pump Energy (J)
C	44.3	200	1.2
N	32	250	2.0
O	24	420	6.5
Ne	14.6	500	9.6
Na	11.9	620	15
Mg	9.9	690	20
Al	8.3	710	21
Si	7.1	870	33

Table 2.2: Results for low-Z elements with $\tau = 50$fs and $\rho = 10^{20}cm^{-3}$

was assumed to have a pulse width $\tau = 50$fs and a line focus of 1cm $\times$ 10μm. Murname [40] observed a peak plasma temperature of 230 eV from a laser-produced plasma using a 160 fsec pulse laser with a cumulative energy flux on target of 300 J/cm^2. If we extrapolate Eqn. 2.9 to a pulse width of 50 fs then a 230 eV plasma can be produced with a flux of 170 J/cm^2 on target. Given a line focus of 1cm $\times$ 10μm and if we assume an efficiency of only 10%, an incident laser with energy of 1.7 J and pulse width of 50 fsec is required. With this we have a relationship between the maximum blackbody temperature and the required laser pump energy to achieve it.

In Table 2.2 the required laser energy for a 50 fsec pulse is given for the corresponding plasma temperature requirement to achieve ISPI x-ray lasing for various low-Z elements. It can be seen that an equivalent blackbody temperature of the x-ray source must be of the order 500 eV, requiring a driving laser with energy of order 10 J or greater, to produce inner-shell photoionized x-ray lasers in the 5 to 15 Å wavelength regime. Results

for C at 45 Å indicate a driving laser with energy of order 1 J is sufficient to produce a large gain-length product. Gains of over 10cm^{-1} can be achieved for C at a density of $1.0 \times 10^{20}\text{cm}^{-3}$ using a 0.5 μm LiH filter and a maximum blackbody temperature of 200 eV pumped with 50 fsec rise time. Collisional ionization to the lower lasing levels limits the duration of lasing giving a pulse width on the order of 40 fsec FWHM. Many approximations are hidden in this model as well as an assumed efficiency. Thus a detailed analysis is required. Current USP laser systems can operate at high power with sub-100 fs pulses and lasers with energies greater than 1J making this scheme realizable in the near term.

Chapter 3

Target Considerations

The required large flux of ionizing x rays used to pump the inner-shell photoionized (ISPI) x-ray laser scheme is obtained from a high-Z target heated by an USP high-intensity optical laser. A high-pass x-ray filter is required between the x-ray source and the lasant to remove low energy x rays, that would lead to significant L-shell ionization. In section 3.1 I discuss high-Z target requirements regarding design and absorption. The needed effectiveness of the high-pass filter and methods of how this can be achieved are addressed in section 3.2.

3.1 Target Design

Figure 3.1 shows our proposed x-ray laser target with a line focused laser beam incident on a high-Z material. Due to the USP nature of the ISPI x-ray laser a traveling wave pump [41] is needed to achieve a large gain length. Output in a single direction is achieved in this manner and the length of the laser is then only dependent on the driving laser and

tolerances in the optical system. This laser-produced plasma emits a broad spectrum of x rays. A high-pass x-ray filter is required to remove low energy x rays, which would lead to significant L-shell ionization. There are two main choices for the high-Z target. A flat target or a structured target can be used. The advantages of using a flat target are the ease of preparation and simplicity of design. However, to achieve high absorption of the incident driving laser energy a large incident angle with p-polarized light must be used. The absorption mechanism is through not-so-resonant resonant absorption [42] where the large absorption rate is accounted for by the electrons being pulled into the vacuum and accelerated back into the plasma. Yet, with this configuration there is a concern that a large fraction of the energy will result in the production of energetic electrons and not into the required source of high energy incoherent x rays. Experimental work compared with simulations has shown absorptions of 60% with 10% of the energy being put into hot electrons [43]. However, as shown in section 4.2 a flat target composed can yield an x-ray drive with sufficient rise time and intensity to drive the inner-shell photoionization x-ray laser scheme.

Structured targets have been shown to result in larger absorption and greater conversion efficiency than to flat targets [44]. Structured targets can be composed of grooves, clusters or cylinders. All of these result in high absorption of the incident energy ($\sim$100% absorption) and high x-ray emission. Cluster targets, e.g., ultra-low density gold or gold-black, are inexpensive but hard to model and have a tendency to build up on the vacuum vessel walls. There are issues of slower rise times associated with potential low density emission [45], as shown in section 4.1. Grooved targets, in general, are expensive but easy

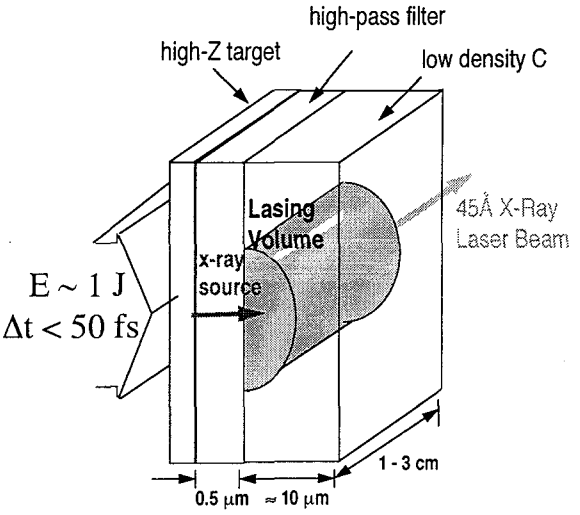

Figure 3.1: The required large flux of x rays is obtained from a high Z target heated by a high-intensity ultrashort-pulse laser. The incoherent filtered x-ray source creates a population inversion in the low density C resulting in x-ray lasing at 45Å.

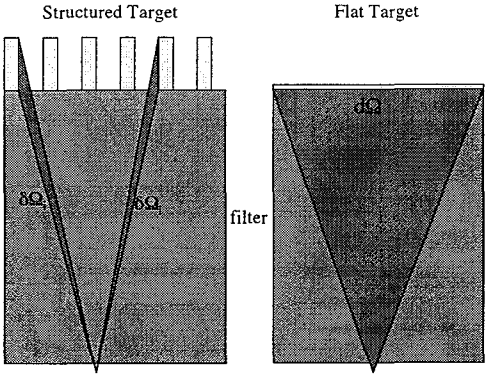

Figure 3.2: The structured target is composed of many small radiators. Each radiating normal to its surface and thus only a fraction of the emission reaches the lasant. We model the difference in radiation incident on the lasant by dividing by a factor of three.

to model. We have modeled the emission from grooved targets assuming absorption in an optical skin depth [46]. However, as seen in fig 3.2 the source is composed of many small radiators and the geometry of the source must be considered since the emission is not uniform over the surface. A third choice is a two-dimensional lattice of cylindrical absorbers where work done by Marjoribanks, et al. [47] shows high x-ray conversion efficiencies for such structured targets. This target is composed of vertical cylinders with diameters from 250 Å to 1000 Å on a substrate. We model the system by considering individual cylinders and calculate the emission normal to the surface. Here also, the energy is assumed deposited in an optical skin depth and the atomic kinetics are calculated with an average-atom atomic model that includes spin-orbit coupling.

For the structured target, we can estimate the radiation emitted from the front side or the backside, through a thin base, by considering the solid angle seen by the lasant. If we consider a structured target as a composition of vertical radiators each emitting uniformly, we have a sum over these radiators. This is somewhat complicated by the fact that each one is a rapidly expanding plasma with varying optical depth. To simplify this we assume the structured emission as the normal emission divided by 3 to account for geometrical effects.

3.2 Filter Requirements

Filtering of the incoherent x-ray source must take place to achieve high gains. In section 2.1 we investigated the needed energy to achieve x-ray lasing by inner-shell photoionization. To estimate this we assumed there was no pumping to the lower-laser level. Of course, this pumping occurs in a real source. However this photoionization can

be essentially eliminated by using a filter. Geometrical effects associated with the plasma being a line source of finite transverse extent and with the separation between the plasma and the lasant given by the filter thickness are included in our calculations.

A low-Z filter can be chosen to optimize the ratio of the x rays at K-shell energies to x rays at the L-shell energies in the lasant. Filtering is primarily through K-shell ionization of the low-Z filter element. For Ne it was found that 3.5 μm of Be with $E_K = 118.4$ eV yield maximum gain. In C, we find that 0.5 μm of Li with $E_K = 59.9$ eV is optimal. This thickness does result in a reduction of x rays at the K edge of C by 25%. However this is required to sufficiently reduce the amount of lower energy x rays. There are windows of high transmission below the filter's K-edge energy and a trade-off is made between filtering at the lasant's K edge to reduce the low energy photons enough for lasing to occur. By a similar approach a high-Z target can be used where M-shell ionization provides the required filtering. A 0.1 μm filter of Ti can provide the required filtering to achieve high gain in C.

A simple measure of the low energy filtering effectiveness of a material may be estimated by the integral of the transmission, T, and the L-shell cross section, σ_L, i.e.,

$$\int_0^\infty \sigma_L(E)T(E)dE$$

By this measure, a thickness of 0.5 μm of LiH and 0.3 μm of Be provide the same amount of filtering for L-shell ionization in C. The Be filter provides twice as much undesired high energy filtering as LiH. Also, 0.1 μm of Ti provides a similar amount of L-shell filtering.

In addition to a layered target-filter approach the self-filtering properties of a material could be utilized. In this approach a slab target is used, the front is heated and the back-side emission from the heated fraction of the solid is filtered by the remaining cold

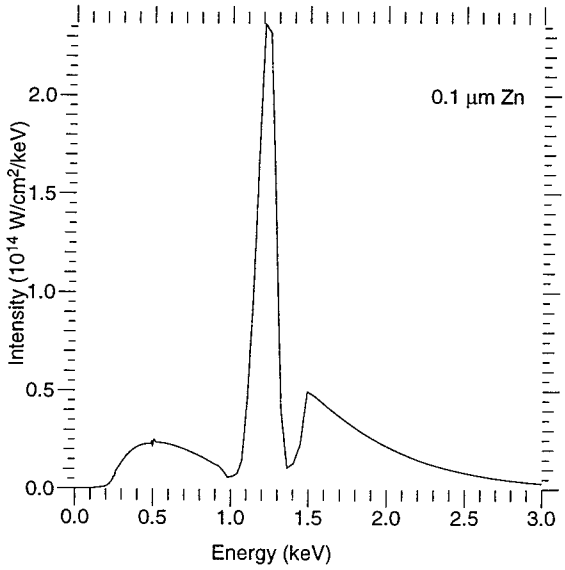

Figure 3.3: The spectral back-side emission is shown for Zn at time of maximum x-ray emission. The effect of filtering can be seen in the reduction of x-ray intensity at energies below 0.3 keV.

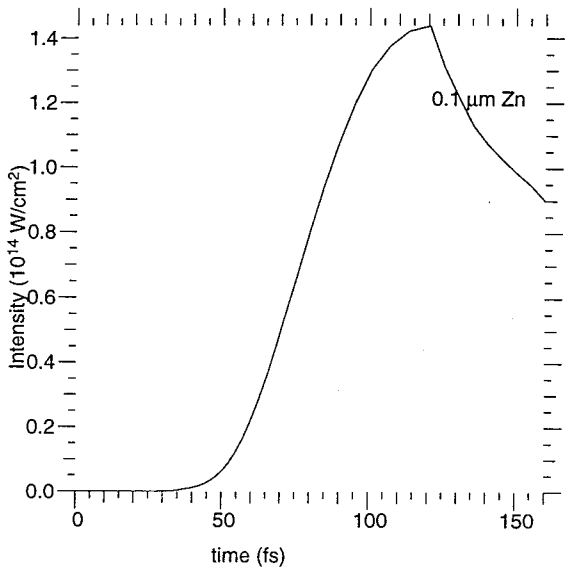

Figure 3.4: The rapid rise time of the self-filtered Zn source is shown.

material. Reasonable gain can be achieved in C Using $\sim 0.1\mu$m of Cu or Zn. However, there remains a significant amount of low energy x rays which can produce an L-shell hole reducing the gain. Figure 3.3 shows the back-side emission spectrum at time of peak emission for a 40 fs, 0.5×10^{17}W/cm^2 of absorbed laser energy incident on a 0.1μm Zn target. For Zn the target has a strong line emission around 1 keV making this a better suited drive for Ne. As shown in Figure 3.4 the rise time of the incoherent x-ray pulse has a sufficiently rapid rise time and large intensity to drive an ISPI x-ray laser.

Chapter 4

The Incoherent X-Ray Drive

Reliable predictions of the gain expected from such an x-ray laser requires an accurate model of both the spectral emission and the rise time of the pump source. In this chapter we present modeling results of the back-side emission from filtered gold targets heated by an USP high intensity laser. We show that this emission produces a short pulse of incoherent high energy x rays and can be used to pump an ISPI x-ray laser. In section 4.1 we investigate limitations on the rise time of the energetic x rays. In sections 4.2 and 4.3 results from modeling are presented showing the fast rise time of the high energy x rays and demonstrating that an USP laser-produced plasma can achieve ISPI lasing in C at 45Å.

4.1 Rise time of the X-Rays

In this section we investigate the rise time of an instantaneously heated source. Modeling using the hydrodynamics/atomic kinetics code LASNEX [35] was done for solid and fractional density Au targets heated uniformly and instantaneously to an electron tem-

perature of 600 eV. The temperature is representative of the electron temperature from a 1 J, 40 fs pulse at peak intensity, see Fig. 4.4. Since in this idealized experiment the interest is in determining the rise time for a particulat density, I did not include hydrodynamic expansion.

One can see in Fig. 4.1 that for solid density Au emission reaches 80% of its maximum value in 16 fs for 300 eV photons and 23 fs for 1 keV photons and for half solid density Au emission reaches 80% of its maximum value in 34 fs. The low energy photons have a fast rise time, i.e., for 300 eV photons the 80% mark is reached in 29 fs compared to 40 fs for 1 keV photons, yet the high energy photons have a higher intensity during the short duration pulse. Thus in going to shorter and shorter pulse widths one must be aware that a limit in the rise time of the incoherent x-ray source exists.

In section 4.2 back-side emission reached 80% of its maximum value in $\sim$ 30 fs, see Fig. 4.5, where the majority of absorption took place at 1/2 solid density. Convergent values for the intensity integrated over a 200 eV range is given in table 4.1 for both solid and half-solid density Au for the ranges centered on 300 eV and 1 keV. If we consider equal mass then the intensity of the 1/2 density Au will be up by a factor of two and similar flux will be observed; however, the rise time will still be slower for the less dense material. Thus, it is crucial to achieve absorption in as near to solid density as possible to achieve rise times below 50 fs.

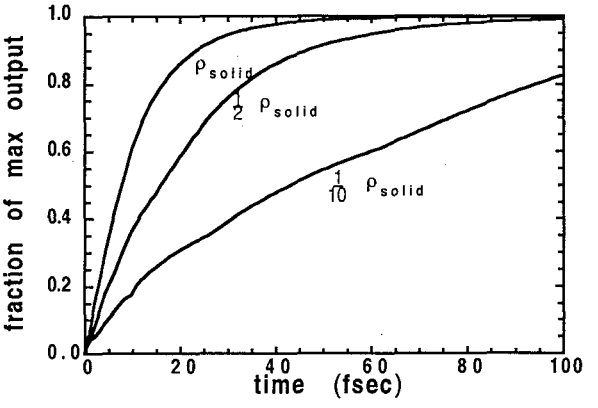

Figure 4.1: A comparisino of the x-ray rise time and output from solid, half-solid and 1/10 solid density Au targets instantaneously and uniformly heated to 600 eV shows the need for a near solid density plasma.

$\int_{E_{min}}^{E_{max}} I(E)dE$	ρ_{solid}	$\frac{1}{2}\rho_{solid}$
E_{min}–E_{max} (eV)	Intensity $\left(\frac{TW}{cm^2}\right)$	
200–400	38.4	17.2
900–1,100	97.2	39.3

Table 4.1: Maximum intensity in the ranges 200-400 eV and 0.9-1.1 keV for solid and half solid density Au from instantaneously heated (electron temperature = 600 eV) 500 Å diameter rods.

4.2 The X-Ray Source

An investigation of the rapid rise time of incoherent x-ray emission from targets heated by an ultra-short pulse (USP) high-intensity optical laser is conducted for use as the x-ray source for inner-shell photoionized (ISPI) x-ray lasing. A line source with the difference in energy with the lasant's K edge being within the L-shell energy would provide maximum coupling of x-ray energy to the lasant atoms, because the cross section is peaked at threshold. In addition, such a line source would effectively reduce electron ionization of the L shell from photoionized electrons.

Modeling using the hydrodynamics/atomic kinetics code LASNEX [35] of a USP driving laser with high intensity incident on a flat target of thin Au layered on a Be filter is presented. The filter has a modest influence on the x-ray emission of the Au via conduction cooling but has a large effect on the backside spectrum by removing low energy x rays as the Au emission passes through the filter. The use of such a filtered source is shown to provide the required x-ray flux to achieve high gain in C at 45 Å.

As seen in Fig. 4.2 a high intensity short pulse laser is incident on a thin Au target layered on a Be filter. The USP laser is absorbed by the Au creating a near-solid density plasma. The laser-produced plasma emits a broad-band spectrum of x rays. However, by the use of a filtered source we are able to reduce the flux of low-energy x rays creating a short duration high-energy x-ray pulse with a rapid rise time. This x-ray source can be used to pump an inner-shell photoionized x-ray laser.

In Fig. 4.3 we show typical spectral results from a 40 fs USP driving laser with an intensity of $1.0 \times 10^{17} \mathrm{W/cm^2}$ incident on a flat target of thin (200Å) Au layered on a

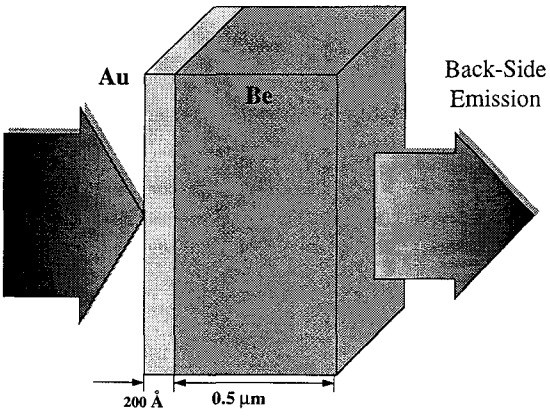

Figure 4.2: A high-intensity USP driving laser is incident on a flat target of thin Au layered on a Be filter, the resulting filtered back-side emission is a short pulse of high-energy x rays.

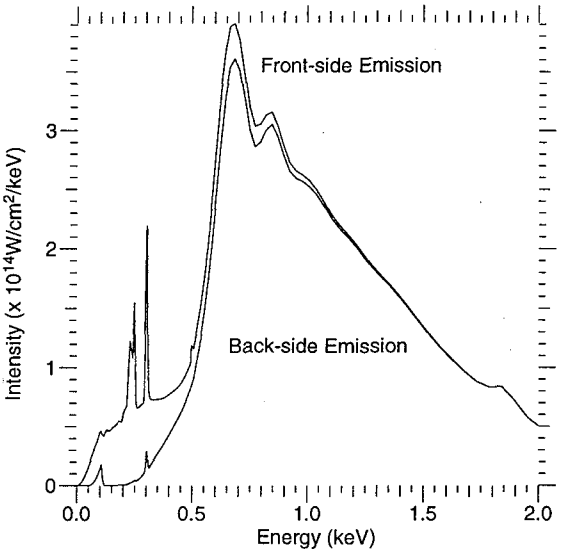

Figure 4.3: The spectral front-side and back-side emission is shown at time of maximum x-ray emission. The effect of filtering can be seen in the reduction of x-ray intensity at energies below 0.5 keV. The intensity is maximum at $\sim$ 0.6 keV.

0.5μm Be filter (see Fig. 4.2). When we model this system, the energy is deposited in a self consistent manner by solving the wave equation for the laser electro-magnetic field [48] and the atomic kinetics and x-ray emission are calculated with an average-atom atomic model that includes spin-orbit coupling. Figure 4.3 shows the effect of filtering and the 0.5μm Be filter reduces the x-ray flux at the carbon K-edge (280 eV) by 75% where filtering is not desired.

The density profile of the Au at the time of maximum USP driving laser intensity is shown in Fig. 4.4 along with the energy deposition rate. The majority of the absorption takes place at half-solid density. The corresponding electron temperature is shown in the plot on the right. A temperature gradient is seen across the Au. At later time, before maximum x-ray emission $\sim$ 100fs, the Au heats uniformly and heats a small portion of the

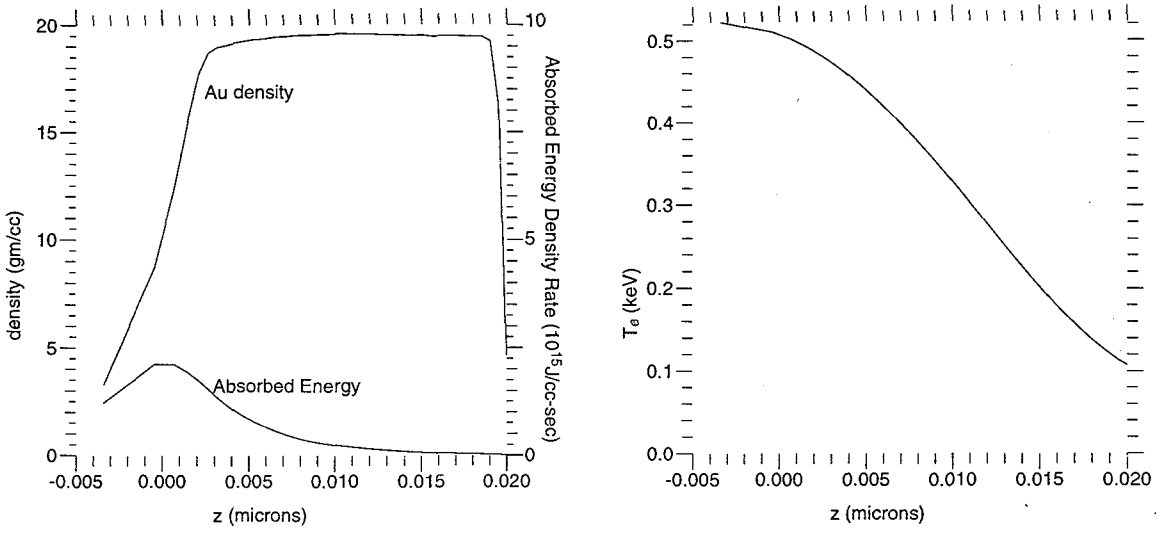

Figure 4.4: Density and absorption of the 200 Å Au target is shown at time of maximum incident laser intensity and the associated electron temperature for a 1.0×10^{17}W/cm^2, 40 fs USP driving laser incident on a flat target of thin (200 Å) Au layered on a 0.5μm Be filter.

Be filter ($\sim$ 100 Å at time of maximum x-ray emission). As seen in Fig. 4.3 low-energy x-ray emission from the front side of the target is significantly greater then the emission from the back side. With the use of a filtered target we are able to reduce the flux of low energy x rays and retain a majority of the high-energy x rays. In Fig. 4.5 the time dependent laser intensity is shown along with the back-side emission. The USP driving laser intensity is shown to precede the back-side x-ray emission by $\sim$ 50fs and have a conversion efficiency of 0.8%. The x-ray pulse consists mainly of x rays above 0.5 keV with a pulse width of $\sim$ 100fs.

4.3 Structured Target Emission

LASNEX modeling of an isolated Au rod of diameter 600 Å with energy deposited within an optical skin depth show that a driving laser requirement of 1 J with a rise time

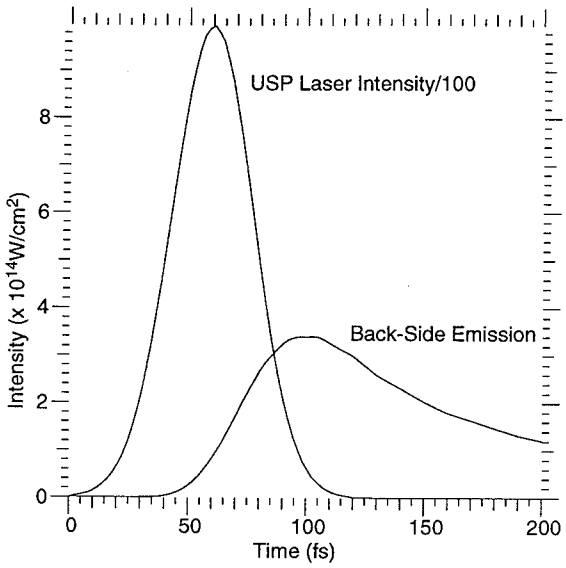

Figure 4.5: The rapid rise time of the filtered source is shown. The incident USP laser pulse precedes the generated x-ray pulse by $\sim$ 50 fs.

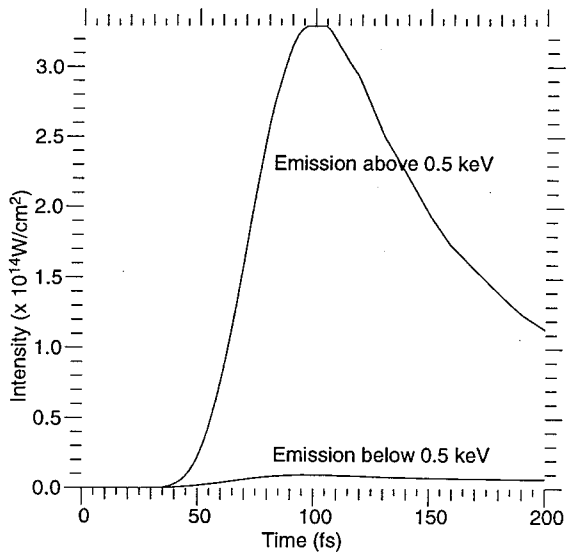

Figure 4.6: The effect of filtering can be seen in the reduction of x-ray intensity below 0.5 keV. The rapid rise time of the high-energy x rays is shown to be $\sim$ 50 fs.

of 40 fs gives a comparable source to the flat target discussed in section 4.2, yet requires less drive energy to produce the needed source. Figure 4.7 shows the emission at time of maximum x-ray emission. As seen in Figure 4.7 the emission spectrum has strong line emission around the C K-edge. The emission convolved with the cross section determines the rate at which photo ionization occurs. Therefore it is optimal to have large emission at or just above the K-edge in order to reduce the needed energy required to drive the ISPI scheme.

Modeling shows that a driving laser with energy of 1 J, with a pulse width of 40 fs FWHM, incident on a structured target composed of vertical cylindrical absorbers (d = 600 Å) is sufficient to produce a large gain-length product. For a 10μm $\times$ 1cm line focus, a density of 1.2×10^{20}cm^{-3}, and a $0.5\mu m$ lithium hydride filter a gain of 15.6cm^{-1}

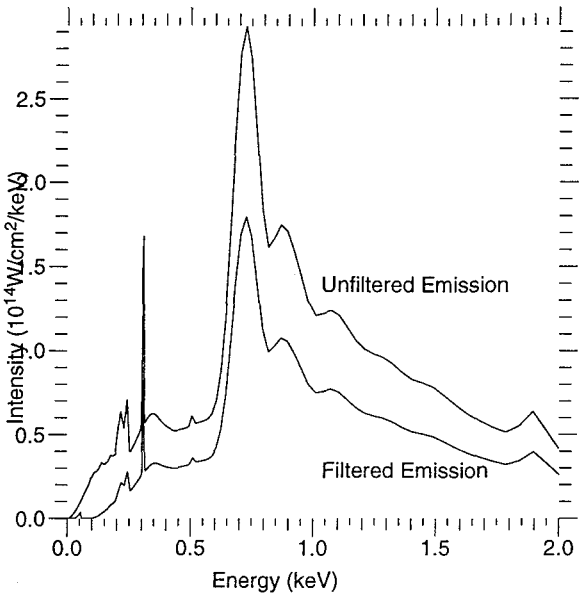

Figure 4.7: A high-intensity USP driving laser is incident on a 600 Å diameter Au rod target, the resulting emission and emission through a 0.5μm LiH filter is shown.

is found. In Fig. 4.8 we show the gain as a function of time along with the time dependent filtered intensity of the x-ray source. The duration of the x-ray source is three times that of the positive gain and the peak gain takes place before the peak of the incoherent x-ray drive and has a rise time of approximately 60 fs. Also shown in the figure the USP optical laser intensity preceeds the incoherent x-ray emission by greater than 50 fs. Collisional ionization to the lower-lasing levels limits the duration of lasing to of order 40 fs FWHM. The self-terminating mechanism of this laser is from electron collisional ionization and the duration of positive gain is dependent on the density of the lasant. While reducing the density lengthens the duration of lasing it also reduces the gain.

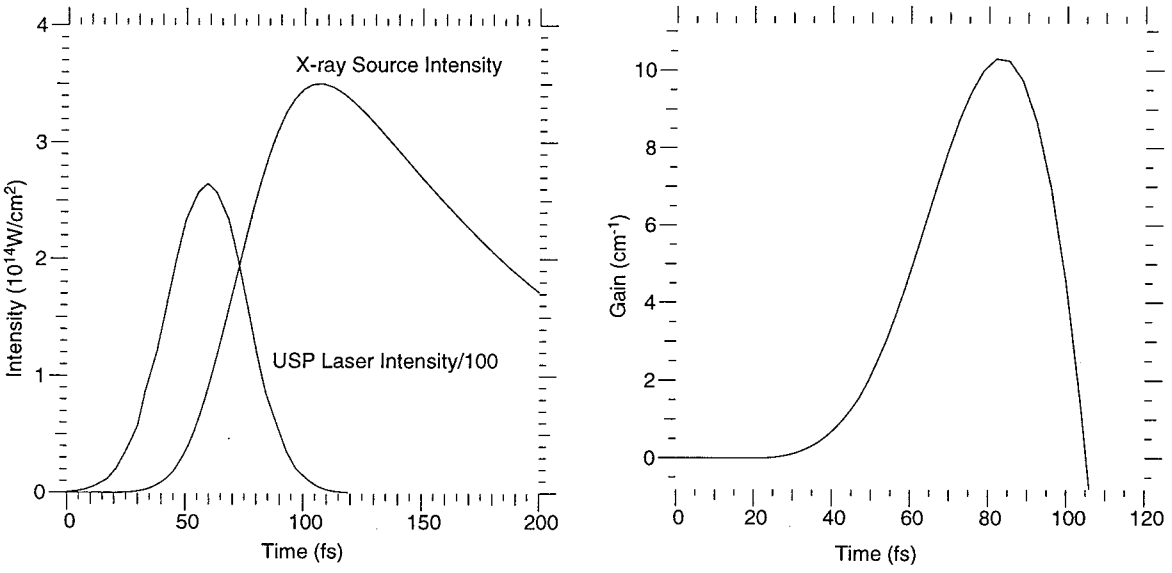

Figure 4.8: The gain as a function of time along with the time dependent optical USP laser intensity divided by 100 and the filtered intensity of the x-ray source are shown.

Chapter 5

Ultrashort-Pulse Coherent X-Ray Source

5.1 X-Ray Lasing in Carbon at 45 Å

We present results, using the conventional ISPI scheme, for C at 45Å as a representative low-Z element where lasing can be tested using current high energy USP lasers. Although current x-ray lasers using Ni-like ions operate at above and below the wavelength considered here, 45 Å, they require high energy (E > 1 kJ) driving lasers [49]. As a result of using a lower energy driving laser (E $\approx$ 1 J), an inner-shell x-ray laser would operate at a higher repetition rate, albeit with less energy in each x-ray pulse. Despite a very short lasing duration (Δt < 100 fs) and small cross sectional area (A $\approx 10^{-6}\text{cm}^2$), the large saturation intensity, I_{sat}, associated with the relatively large Auger rate out of the upper lasing state [38] results in significant energy per pulse yielding a high average energy.

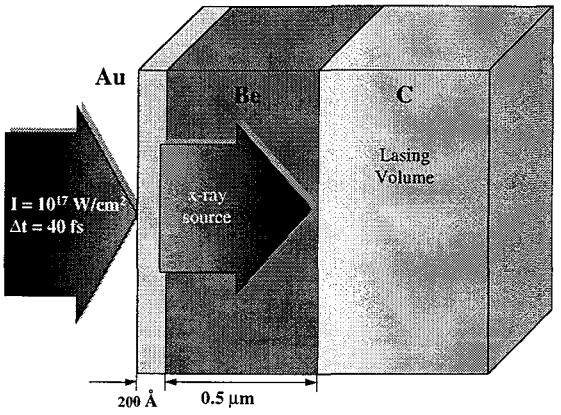

Figure 5.1: The required large flux of x rays is obtained from a high Z target heated by a high-intensity ultrashort-pulse laser. The incoherent filtered x-ray source creates a population inversion in the low density C resulting in x-ray lasing at 45Å.

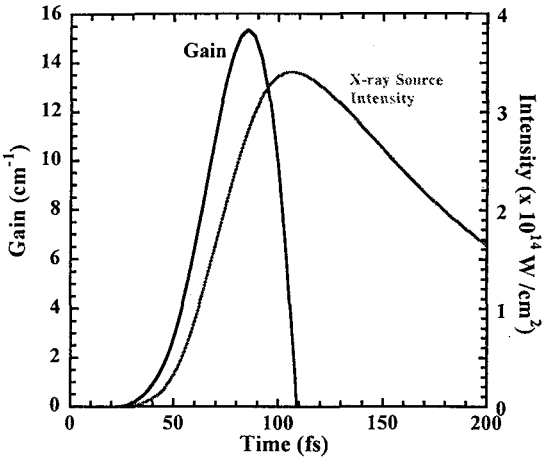

Figure 5.2: The gain as a function of time along with the time dependent optical USP laser intensity divided by 100 and the filtered intensity of the x-ray source are shown.

Figure 5.1 shows our proposed x-ray laser target with a line focused laser beam incident on a high-Z material. This laser produced plasma emits a broad spectrum of x rays. A high-pass x-ray filter is required to remove low energy x rays, which would lead to significant L-shell ionization, prior to the x-ray source being incident on the low density C. Modeling shows that a driving laser of intensity 10^{17}W/cm^2, 40 fs FWHM, incident on a flat target composed of 200Å Au layered on a 0.5μm Be filter is sufficient to produce a large gain-length product. For a 10μm $\times$ 1cm line focus, a carbon density of 1.2×10^{20}cm^{-3}, a peak gain of 15.6cm^{-1} is found. In Fig. 5.2 we show the gain as a function of time along with the time dependent filtered intensity of the x-ray source. Collisional ionization to the lower-lasing levels limits the duration of lasing to $\sim$ 50 fs FWHM.

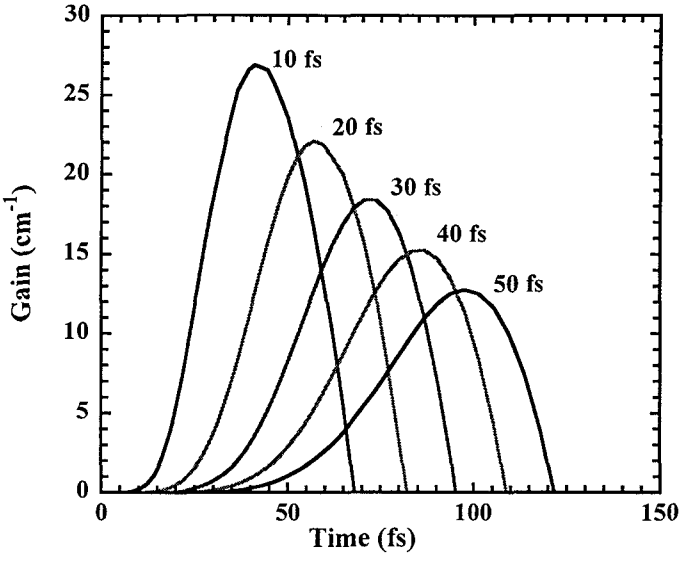

Figure 5.3: The calculated gain coefficient depends on the input pulse duration and we show the effect of changing the pulse duration from 50 to 10 fs FWHM for a constant density of $1.2 \times 10^{20}\text{cm}^{-3}$ and a constant energy source of 1 J.

5.2 Lasant

The required low neutral carbon density of order 10^{20}cm^{-3} can be achieved using a number of different approaches. In low density carbon foam the average cluster size is on the order of 100Å. While the clusters have much higher local densities, where energetic electrons have a mean free path on the order of angstroms, a prepulse can be used to heat the clusters causing them to expand filling the voids and creating a uniform low density target. Alternatively, the use of a methane gas jet can also provide the required densities of Carbon. Dissociation of the methane molecule does not take place on the time scale of x-ray lasing. Therefore, the lasing photons are from the molecular transition $(1a_1)^{-1}$ to $(1t_2)^{-1}$ which has similar energy and line width as the 2p-1s atomic transition [50, 51].

The calculated gain coefficient depends on the pulse duration as shown in Fig. 5.3

where the pulse duration was varied from 50 to 10 fs FWHM. We find an increase in the gain from 13 to 28 cm^{-1} as the pulse duration is reduced from 50 to 10 fsec. The resulting gain widths are similar ~40 fs FWHM. Allowing for absorption, the effective gain is $\sim 23cm^{-1}$ for a 10 fs, $\sim 10cm^{-1}$ for 40 fs and zero for pulses longer than 80 fs. Thus, a 40 fs FWHM USP laser with twice the energy can obtain a similar *gl* to a 10 fs laser, yet a laser with a pulse length longer than 80 fs can not achieve x-ray lasing at any power.

Our calculations show that a driving laser with a pulse duration of 40 fs, a $10\mu m \times$ 1cm line focus, and energy of 1 J gives a gain length of 15.6 in C at 45Å or an effective gain length of 10 accounting for absorption. We demonstrate that such a short duration for the optical driving pulse is required to control collisional filling of the lower laser state. Optical lasers with the required attributes and with repetition rates of order 10 Hz are becoming available, making this approach realizable in the near term.

Chapter 6

Conclusion

Theoretical work on inner-shell photoionized x-ray lasers in the 45 Å to 15 Å or less wavelength regime requires a driving laser with energy of order 1 J to 10 J or greater. Our results for C at 45 Å show that a driving laser with energy of order 1 J is sufficient to produce a large gain-length product. Gains of over 10cm^{-1} were found for C with a density of $1.0 \times 10^{20}\text{cm}^{-3}$ using a 0.5 μm LiH filter pumped with 40 fs 1 J USP laser incident on a structured Au target. Collisional ionization to the lower lasing levels limits the duration of lasing giving a pulse on the order of 50 fsec FWHM.

The laser produced plasma emits a broad spectrum of x rays. A high-pass x-ray filter is required to remove low energy x rays, which would lead to significant L-shell ionization, prior to the x-ray source being incident on the low density C. Significant gain can not be achieved without filtering and the filtering of low energy x rays also results in the reduction of x rays at and above the K-edge by 25% where filtering is not desired. During the time of positive gain, the ionization front has penetrated the Au and 0.04μm

of the filter. This reduction in effective filter thickness of less than 10% does not lead to significant changes in gain but is included in our model. We have investigated the use of 0.1μm Ti as a filter layered on Au and performed back-side emission calculations from micron thick targets of Cu which self filter low energy x rays. We find that these targets also provide the needed emission to achieve high gain in C at 45Å.

As discussed in chapter 4 the low-energy x rays can be significantly reduced by filtering techniques and the rise time of these energetic x rays is quite fast. The rise-time limitations of these targets was investigated by uniformly and instantaneously heating a solid Au target to 600 eV. Emission for solid density Au reached 80% of its maximum value in 18 fs and for half solid density Au emission reached 80% of its maximum value in 34 fs. Thus in going to shorter and shorter pulse widths one must be aware that a limit in the rise time of the incoherent x-ray source exists.

X-ray emission from the back-side of a filtered target of thin (200 Å) Au layered on a 0.5μm Be filter heated by a 40 fs FWHM USP high-intensity, 10^{17}W/cm^2 optical laser has been shown to produce a short pulse (88 fs FWHM) of high-energy x rays with a conversion efficiency of 0.8%. Our calculations show that a driving laser with a pulse duration of 40 fs, a 10μm $\times$ 1cm line focus, and energy of 4 J gives a gain length of 15.6 in C at 45Å or an effective gain length of 10 accounting for absorption. We demonstrated that such a short duration for the optical driving pulse is required to control collisional filling of the lower laser state.

I have shown the promise of ISPI x-ray lasing. This scheme was one of the first proposed x-ray laser schemes and it has been the most difficult to get working. However,

with the advent of USP lasers within the 10–50 fs region and with energies > 1 J there is promise that x-ray lasing can be achieved via inner-shell photoionization.

Bibliography

[1] D. L. Matthews, P. L. Hagelstein, M. D. Rosen, M. J. Eckart, N. M. Ceglio, A. U. Hazi, H. Medecki, B. J. MacGowan, J. E. Trebes, B. L. Whitten, E. M. Campbell, C. W. Hatcher, A. M. Hawryluk, R. L. Kauffman, L. D. Pleasance, G. Rambach, J. H. Scofield, G. Stone, and T. A. Weaver. Demonstration of a soft x-ray amplifier. *Physical Review Letters*, 54(2):110–113, 1985.

[2] B. J. MacGowan, S. Maxon, L. B. Da Silva, D. J. Fields, C. J. Keane, D. L. Matthews, A. L. Osterheld, J. H. Scofield, G. Shimkaveg, and G. F. Stone. Demonstration of x-ray amplifiers near the carbon K edge. *Physical Review Letters*, 65(4):420–423, 1990.

[3] J. Zhang, A. G. MacPhee, J. Lin, E. Wolfrum, R. Smith, C. Danson, M. H. Key, C. L. Lewis, D. Neely, J. Nilsen, G. J. Pert, G. J. Tallents, and J. S. Wark. A saturated x-ray laser beam at 7 nanometers. *Science*, 276(5315):1097–1100, 1997.

[4] James Dunn, Albert L. Osterheld, Ronnie Shepherd, William E. White, Vyacheslav N. Shlyaptsev, Anthony B. Bullock, and Richard E. Stewart. Table-to ptransient collisional excitation x-ray laser research al LLNL. In *SPIE Proceedings*, volume 3156, pages 114–121, San Diego, CA, July 1997. SPIE.

[5] P. Jaeglé, S. Sebban, A. Carillon, G. Jamelot, A. Klisnick, P. Zeitoun, B. Rus, F. Albert, and D. Ros. X-ray laser progress and applications experiments at LULI. In S. Svanberg and C-G Wahlström, editors, *X-Ray Lasers 1996*, 151, pages 1–8, Bristol, UK, 1996. Institute of Physics.

[6] E E Fill, K Eidmann, Y Li, P X Lu, and G Pretzler. Experiments towards X-ray lasers and applications. In S. Svanberg and C-G Wahlström, editors, *X-Ray Lasers 1996*, 151, pages 25–31, Bristol, UK, 1996. Institute of Physics.

[7] M H Key, T W Barbee Jr, J W Blyth, K Burnett, G F Cairns, A E Dangor, T Ditmire, A Djaoui, L B Da Silva, A Demir, A Dyson, A P Fews, E E Fill, P Gibbon, P Lee, S Healy, M Holden, M H R Hutchinson, D H Kalantar, N S Kim, C L S Lewis, Y Lin, P Loukakos, A G McPhee, I Mercer, S Moustaizis, M Nakai, D Neely, P Norreys, A A Offenberger, G J Pert, S G Preston, B A Remmington, A Sanpera, D Schlogl, C G Smith, R Smith, J Steingruber, G J Tallents, F Walsh, J S Wark, J Warwick, E Wolfrum, M Zepf, P Zeitoun, and J Zhang. Development and applications of ultra-bright laser and harmonic XUV sources. In S. Svanberg and C-G Wahlström, editors, *X-Ray Lasers 1996*, 151, pages 9–16, Bristol, UK, 1996. Institute of Physics.

[8] D. L. Matthews. Possibility of short wavelength x-ray lasers and their applications. In S. Svanberg and C-G Wahlström, editors, *X-Ray Lasers 1996*, 151, pages 32–39, Bristol, UK, 1996. Institute of Physics.

[9] Y. Nagata, K. Midorikawa, S. Kubodera, M. Obara, H. Tashiro, and K. Toyoda. Soft-

x-ray amplification of the lyman-alpha transition by optical-field-induced ionization. *Phys. Rev. Lett.*, 71:3774–3777, 1993.

[10] Y. Nagata, K. Midorikawa, S. Kubodera, M. Obara, H. Tashiro, K. Toyoda, and Y. Kato. *Phys. Rev. A*, 51:1415, 1995.

[11] D. C. Eder, P. Amendt, L. B. DaSilva, R. A. London, B. J. MacGowan, D. L. Matthews, B. M. Penetrante, M. D. Rosen, S. C. Wilks, T. D. Donnelly, R. W. Falcone, and G. L. Strobel. Tabletop x-ray lasers. *Phys. Plasmas*, 1(5):1744–1752, 1994.

[12] K. M. Krushelnick, W. Tighe, and S. Suckewer. *J. Opt. Soc. B*, 13:306, 1996.

[13] B. N. Chichkov, A. Egbert, H. Eichmann, C. Momma, S. Nolte, and B. Wellegehausen. *Phys. Rev. A*, 52:1629, 1995.

[14] B. E. Lemoff, G. Y. Yin, C. L. Gordon, C. P. J. Barty, and S. E. Harris. *Phys. Rev. Lett.*, 74:1574, 1995.

[15] C. P. J. Barty, T. Guo, C. LeBlanc, F. Raksi, C. Rosepetruck, J. Squier, K. R. Wilson, V. V. Yakovlev, and K. Yamakawa. Generation of 18-fs, multiterawatt pulses by regenerative pulse shaping and chirped-pulse amplification. *Opt. Lett.*, 21:668–670, 1996.

[16] I. P. Christov, V. D. Stoev, M. M. Murname, and H. C. Kapteyn. Sub-10-fs operation of kerr-lens mode-locked lasers. *Opt. Lett.*, 21:1493–1495, 1996.

[17] Michael D. Perry and Gerard Mourou. Terawatt to petawatt subpicosecond lasers. *Science*, 264(5161):917–924, 1994.

[18] Gerard A. Mourou, Christopher P. J. Barty, and Michael D. Perry. Ultrahigh-intensity lasers: Physics of the extreme on a tabletop. *Physics Today*, 51(1):22–28, 1998.

[19] P. V. Nickles, V. N. Shlyaptsev, M. Kalachnikov, M. Schnurer, I. Will, and W. Sandner. Short pulse x-ray laser at 32.6 nm based on transient gain in Ne-like titanium. *Phys. Rev. Lett.*, 78:2748, 1997.

[20] B. E. Lemoff, G. Y. Yin, C. L. Gordon, C. P. J. Barty, and S. E. Harris. Femtosecond-pulse-driven 10-hz 41.8-nm laser in Xe IX. *J. Opt. Soc. B*, 13:180–184, 1996.

[21] D. C. Eder. Hydrogenlike magnesium x-ray laser design. *Phys. Fluids B*, 2:3086, 1990.

[22] D. V. Korobkin, CH Nam, S Suckewer, and A. Goltsov. Demonstration of soft x-ray lasing to ground state in Li III. *Phys. Rev. Lett.*, 77:5206–5209, 1996.

[23] J. Dunn, A. L. Osterheld, R. Shepherd, W. E. White, V. N. Shlyaptsev, and R. E. Stewart. Demonstration of x-ray amplification in transient gain nickel-like palladium scheme. *Physical Review Letters*, 1998. submitted 24 Sept. 1997.

[24] S. G. Preston, A. Sanpera, M. Zepf, W. J. Blyth, et al. High-order harmonics of 248.6 nm KrF laser from Helium and Neon ions. *Physical Review A*, 53(1):R31–R34, 1996.

[25] R. Haight and D. R. Peale. Antibonding state on the Ge(111):As surface: Spectroscopy and dynamics. *Phys. Rev. Lett.*, 70:3979–3982, 1993.

[26] T. Ditmire, K. Kulander, J. K. Crane, H. Nguyen, and M. D. Perry. Calculation and measurement of high-order harmonic energy yields in helium. *J. Opt. Soc. B*, 13:406–411, 1996.

[27] J. L. Porter, R. B. Spielmann, M. K. Matzen, E. J. McGuire, L. E. Ruggles, M. F. Vargas, J. P. Apruzese, R. W. Clark, and J. Davis. Demonstration of population inversion by resonant photopumping in a neon gas cell irradiated by a sodium Z pinch. *Physical Review Letters*, 68(6):796–799, 1992.

[28] J. J. Rocca, V. Shlyaptsev, F. G. Tomasel, O. D. Cortázar, D. Hartshorn, and J. L. A. Chilla. Demonstration of a discharge pumped table-top soft-x-ray laser. *Physical Review Letters*, 73(16):2192–2195, 1994.

[29] J. J. Rocca, D. P. Clark, J. L. A. Chilla, and V. N. Shlyaptsev. Energy extraction and achievement of the saturation limit in a discharge-pumped table-top soft x-ray amplifier. *Physical Review Letters*, 77(8):1476–1479, 1996.

[30] V.N. Shlyaptsev, P.V. Nickles, T. Schlegel, M.P. Kalashnikov, and A.L. Osterheld. In *SPIE Proceedings*, volume 2012, page 111, San Diego, CA, July 1993. SPIE.

[31] C. D. Decker and R. A. London. Design for a compact Ni-like-tungsten x-ray laser. *Physical Review A*, 57(2), 1998.

[32] M. A. Duguay and P. M. Rentzepis. Some approaches to vacuum UV and x-ray lasers. *Applied Physics Letters*, 10(12):350–352, 1967.

[33] H. C. Kapteyn. Photoionization-pumped x-ray lasers using ultrashort-pulse excitation. *Applied Optics*, 31:4931–4939, 1992.

[34] G. L. Strobel, D. C. Eder, R. A. London, M. D. Rosen, R. W. Falcone, and S. P. Gordon. In *SPIE Proceedings, Short-Pulse High-Intensity Lasers and Applications II*, volume 1860, page 157, L.A., CA, Jan. 1993. SPIE.

[35] G. B. Zimmerman and W. L. Kruer. Numerical simulations of laser-initiated fusion. *Comments Plasma Phys. Controlled Fusion*, 2(2):51–61, 1975.

[36] Eugene J. McGuire. K-shell auger transition rates and fluorescence yields for elements Be-Ar. *Physical Review*, 185(1):1–6, 1969.

[37] M. O. Krause. Atomic radiative and radiationless yields for K and L shells. *Journal of Physical and Chemical Reference Data*, 8(2):307, 1979.

[38] G. L. Strobel, D. C. Eder, and P. Amendt. Saturation intensity for ultrashort-pulse laser schemes. *Appl. Phys. B*, 58:45, 1994.

[39] A. Caruso and R. Gratton. Interaction of short laser pulses with solid materials. *Plasma Physics*, 11:839–847, 1969.

[40] Margaret M. Murname. *Sub-Picosecond Laser-Produced Plasmas.* PhD thesis, University of California at Berkeley, 1989.

[41] R. A. Snavely, L. B. Da Silva, D. C. Eder, D. L. Matthews, and S. J. Moon. Traveling wave pumping of ultra-short pulse x-ray lasers. In *SPIE Proceedings*, volume 3156, San Diego, CA, July 1997. SPIE.

[42] F. Brunel. Not-so-resonant, resonant absorption. *Phys. Rev. Lett.*, 59:52–55, 1987.

[43] H. Chen, B. Soom, B. Yaakobi, S. Uchida, and D. D. Meyerhofer. Hot-electron characterization from $k\alpha$ measurements in high-contrast p-polarized, picosecond laser-plasma interactions. *Phys. Rev. Lett.*, 70(22):3431–3434, 1993.

[44] M. M. Murname, H. C. Kapteyn, S. P. Gordon, J. Bokor, E. N. Glytsis, and R. W. Falcone. Efficient coupling of high-intensity subpicosecond laser pulses into solids. *Appl. Phys. Lett.*, 62(10):1068–1070, 1993.

[45] S. J. Moon and D. C. Eder. Target considerations for inner-shell photo-ionized x-ray lasing. In S. Svanberg and C-G Wahlström, editors, *X-Ray Lasers 1996*, 151, pages 143–145, Bristol, UK, 1996. Institute of Physics.

[46] D. C. Eder, R. A. London, M. D. Rosen, and G. L. Strobel. In *SPIE Proceedings, Applications of Laser Plasma Radiation*, volume 2015, page 234, San Diego, CA, July 1993. SPIE.

[47] R. Marjoribanks, G. Kulcsár, F. Budnik, L. Zhao, P. Herman, D. Al-Mawlawi, and M. Moskovits. *Bull. Amer. Phys. Soc.*, 39:1519, 1994.

[48] W. E. Alley. A maxwell equation solver for the simulation of moderatley intense ultrashort pulse laser experiments. *ICF Quarterly Rept.*, 2(4):160–165, 1992.

[49] E. E. Fill, editor. *X-Ray Lasers 1992, Proceedings of the 3rd International Colloquium on X-Ray Lasers*, 125, Bristol, UK, 1992. Institute of Physics.

[50] H. Chatham, D. Hils, R. Robertson, and A. Gallagher. Total and partial electron collisional ionization cross sections for CH_4,C_2H_6, SiH_4, and Si_2H_6. *J. Chem. Phys.*, 81(4):1770–1777, 1984.

[51] T. E. Meehan, J. McColl, and F. P. Larkins. Theoretical x-ray emission spectra for fluoromethane molecules following carbon K-shell ionization. *J. Electron Spectrosc. Relat. Phenom.*, 73:283, 1995.

[52] D. A. Verner and D. G. Yakovlev. Analytic fits for partial photoionization cross sections. *Astron. Astrophys. Suppl. Ser.*, 109(1):125–133, 1996.

[53] D. A. Verner, E. M. Verner, and G. J. Ferland. Atomic data for permitted resonance lines of atoms and ions from H to Si, and S, Ar, Ca, and Fe. *ATOMIC DATA AND NUCLEAR DATA TABLES*, 64(1):1–180, 1996.

[54] A.S. Kamrukov, N.P. Kozlov, Yu.S. Protasov, and S.N. Chuvashev. *Opt. Spectr.*, 55:9, 1983.

[55] M. Arnaud and R. Rothenflug. An updated evaluation of recombination and ionization rates. *Astron. Astrophys. Suppl. Ser.*, 60:425–457, 1985.

[56] M. Arnaud and J. Raymond. Iron ionization and recombination rates and ionization equilibrium. *The Astrophysical Journal*, 398:394–406, 1992.

Appendix A

Level Structure and Lasing Transition

In the ISPI scheme, lasing takes place between the L shell and the K shell. The L shell consists of $2p$ and $2s$ states which are split by a few eV's of energy. The lower-laser state is the $2p$ hole state. However, it is important to keep track of the $2s$ state due to electron ionizations. The laser rate equations in the small signal approximation are given below.

$$\dot{N}_0 = -(R_K + R_L + R_L^e)N_0 \tag{A.1}$$

$$\dot{N}_K = R_K N_0 - \frac{N_K}{\tau_K} - (R_{KK} + R_{KL} + R_{KL}^e)N_K \tag{A.2}$$

$$\dot{N}_{L_{2p}} = (R_{L_{2p}} + R_{L_{2p}}^e)N_0 + \frac{N_K}{\tau_{Rad}} - (R_{LL_{2p}} + R_{LK_{2p}} + R_{LL_{2p}}^e)N_{L_{2p}} - \frac{N_{L_{2p}}}{\tau_{L_{2p}}} \tag{A.3}$$

$$\dot{N}_{L_{2s}} = (R_{L_{2s}} + R_{L_{2s}}^e)N_0 - (R_{LL_{2s}} + R_{LK_{2s}} + R_{LL_{2s}}^e)N_{L_{2s}} - \frac{N_{L_{2s}}}{\tau_{L_{2s}}} \tag{A.4}$$

The gain is given by,

$$\mathrm{g} = \sigma_s \left(\mathrm{N_K} - \frac{\mathrm{g_K}}{\mathrm{g_{L_{2p}}}} \mathrm{N_{L_{2p}}} \right) \tag{A.5}$$

where the gain is denoted g, the degeneracies of the upper- and lower-laser levels are denoted g_K and $g_{L_{2p}}$, respectively and σ_s is the stimulated emission cross section. We also take into consideration the additional ionization states.

$$\dot{\mathrm{N}}_{LL} = (R_{LL} + R^e_{LL})\mathrm{N_L} - (\mathrm{R_{Li-like}} + \mathrm{R^e_{Li-like}})\mathrm{N_{LL}} \tag{A.6}$$

$$\dot{\mathrm{N}}_{KL} = (R_{KL} + R^e_{KL})\mathrm{N_K} - (\mathrm{R_{Li-like}} + \mathrm{R^e_{Li-like}})\mathrm{N_{KL}} \tag{A.7}$$

$$\dot{\mathrm{N}}_{KK} = (R_{KK} + R^e_{KK})\mathrm{N_K} - (\mathrm{R_{Li-like}} + \mathrm{R^e_{Li-like}})\mathrm{N_{KK}} \tag{A.8}$$

$$\dot{\mathrm{N}}_{\mathrm{Li-like}} = (R_{\mathrm{Li-like}} + R^e_{\mathrm{Li-like}})\mathrm{N_{LL}} - (\mathrm{R_{He-like}} + \mathrm{R^e_{He-like}})\mathrm{N_{Li-like}} \tag{A.9}$$

$$\dot{\mathrm{N}}_{\mathrm{He-like}} = (R_{\mathrm{He-like}} + R^e_{\mathrm{He-like}})\mathrm{N_{Li-like}} - (\mathrm{R_{H-like}} + \mathrm{R^e_{H-like}})\mathrm{N_{He-like}} \tag{A.10}$$

$$\dot{\mathrm{N}}_{\mathrm{H-like}} = (R_{\mathrm{H-like}} + R^e_{\mathrm{H-like}})\mathrm{N_{He-like}} \tag{A.11}$$

here the photoionization and electron ionization rates are given by R_i and R^e_i, where

$$i \in \{K, L, L_{2p}, L_{2s}, LL, LL_{2p}, LL_{2s}, KL, KK, \tag{A.12}$$

$$\mathrm{Li-like, He-like, and H-like}\} \tag{A.13}$$

When the L state is denoted without the 2p or 2s subscript it is assumed to consists of both 2p and 2s states, i.e.,

$$R_L = R_{L_{2p}} + R_{L_{2s}}$$

The photoionization and electroionization are given by the equations,

$$R_i = \int_0^\infty dE\ \sigma_i(E)\Phi(E) \tag{A.14}$$

$$R^e_i = \int_0^\infty dE\ \sigma^e_i(E)N_e(E)v_e(E) \tag{A.15}$$

where σ_i and σ_i^e are the photoionization and electroionization cross section respectively. Φ is the intensity of the incoherent pump source, $N_e(E)$ is the number density of electrons with energy between E and dE and $v_e(E)$ their respective velocity. In addition to the laser rate equations we also have a rate equation for the electron population. The number of electron induced ionization events is given by,

$$N_I(E) = \sum_i N_e(E) v_e(E) dt \sigma_i^e(E) N_i \tag{A.16}$$

where the sum over i indicates over all ionization states included in eqn. A.13. The rate of electron induced ionization events simplifies to,

$$\dot{N}_I(E) = \sum_i R_i^e(E) N_i \tag{A.17}$$

$$R_i^e(E) = \sigma_i^e(E) N_e(E) v_E(E) \tag{A.18}$$

$$R_i^e = \int_0^\infty R_i^e(E) dE \tag{A.19}$$

N_i is the time dependant population of level i. However, each collision leads to an exchange of energy. If we denote E_0 as the initial energy of the incident particle then,

$$E_0 = E_p + E_t + Q$$

where E_p and E_t is the final energy of the projectile and target electron, respectively and Q is the excitation energy. Since the target and projectile electron are indistinguisable after the collision we assume it has the larger energy and therefore,

$$E_t \leq (E_0 - Q)/2$$

The distribution of energies is determined by the differential cross section, $\Phi(E_t)dE_t$ where

$$\int_0^{(E_0-Q)/2} \Phi(E_t) dE_t = \sigma^e(E_0)$$

If we make assume a dipole transition we can use the normalized photo ionization cross section to distribute the energies.

$$\dot{N}_e(E) = \sum_i R_i(E-Q) + \sum_i \int (R_i^e(E-Q)T(E',E)) \tag{A.20}$$

where E is the energy, Q is the excitation energy and T is a probability function to take into account the distribution of energy between the incident electron and the target electron given by the differential cross section.

A complete set of analytic fits for partial photoionization was found in the work by Verner and Yakovlev [52, 53]. The cross sections are fitted using the analytic formula developed by Kamrukov, et al. [54].

$$\sigma_{nl}(E) = \sigma_0 F(E/E_0)\text{Mb}, \tag{A.21}$$

$$F(y) = [(y-1)^2 + y_w^2]y^{-Q}(1+\sqrt{y/y_a})^{-P} \tag{A.22}$$

where n is the principle quantum number of the shell, $l = 0, 1, 2$ (or s, p, d) is the subshell orbital quantum number. E is the photon energy in eV, $y = E/E_0$; σ_0, E_0, y_w, y_a and P are fit parameters and $Q = 5.5 + l - 0.5P$. These photoionization cross-sections are based on Hartree-Dirac-Slater (HDS) calculations and compared with experiment. For C, the cross sections for neutral and singly ionized are shown in fig A.1. In fig A.2 the total cross section is shown for CII, singly ionized C, and compared with data from the Opacity Project. Very good agreement is achieved for our purposes and the accuracy attained is more than sufficient.

The electron ionization cross sections and rates of direct collisional ionization were fit using analytical fits by Arnaud [55, 56], see fig. A.3.

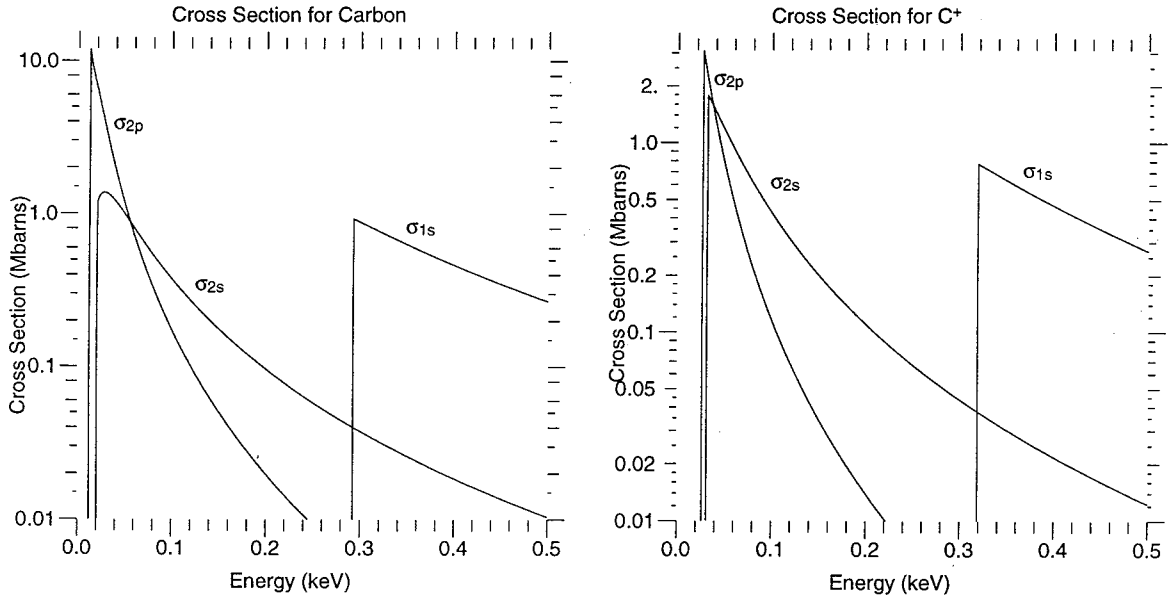

Figure A.1: Partial photoionization cross sections are shown for neutral and singly ionized C.

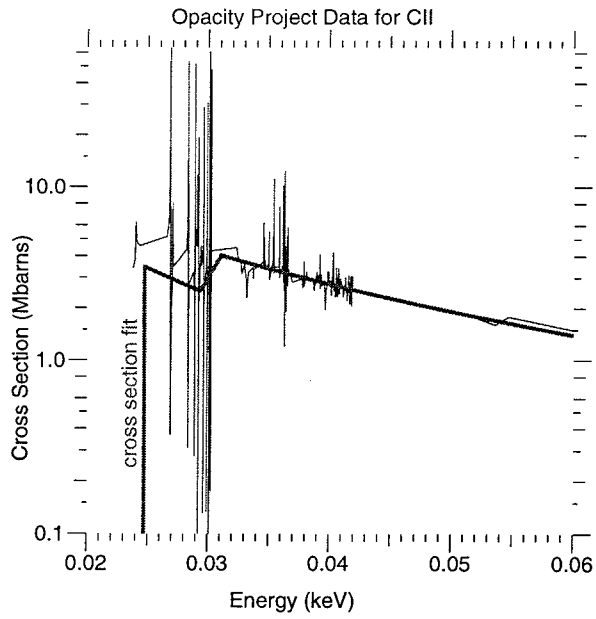

Figure A.2: The total photoionization cross section for singly ionized C is shown with Opacity Project data.

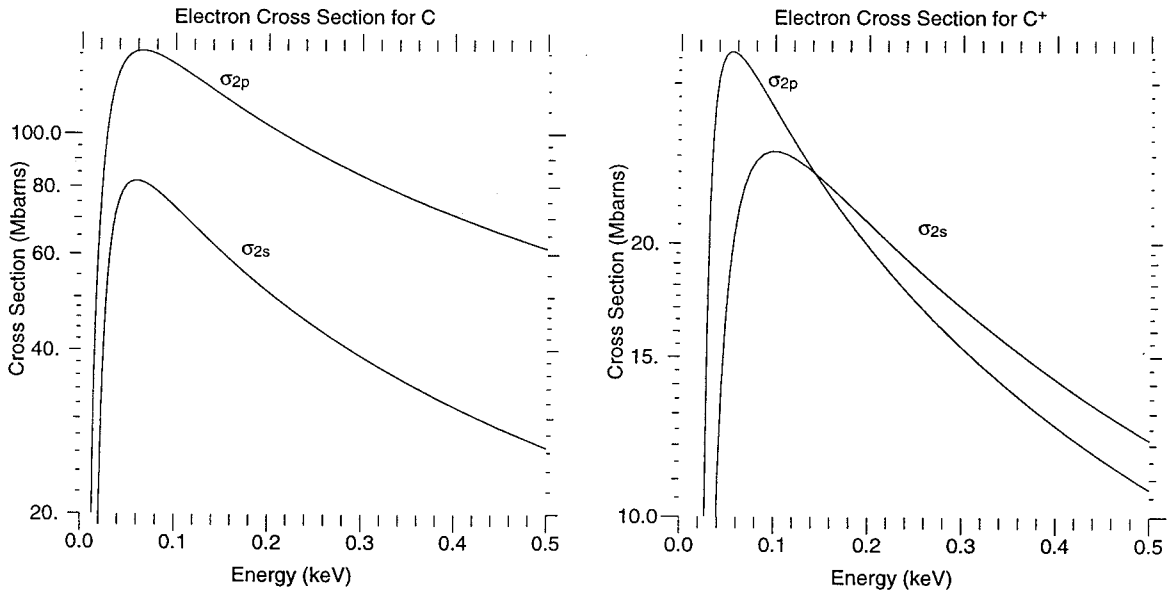

Figure A.3: Partial electron ionization cross sections are shown for neutral and singly ionized C.